Impact of waves on phytoplankton activity on the Northwest European Shelf: insights from observations and km-scale coupled models

Dale Partridge[1,4,*], Ségolène Berthou[2], Rebecca Millington[1], James R. Clark[1], Lucy Bricheno[3], Juan Manuel Castillo[2], Julia Rulent[3], and Huw Lewis[2]

[1]Plymouth Marine Laboratory, Plymouth, PL1 2LP, UK
[2]Met Office, Exeter, EX1 3PB, UK
[3]National Oceanography Centre, Liverpool, L3 5DA, UK
[4]National Centre for Earth Observation, Leicester, LE4 5SP, UK
[*]Corresponding author: Dale Partridge, dapa@pml.ac.uk

Abstract. The spring bloom is an annual event in temperate regions of the North Atlantic Ocean ~~in which~~ where the abundance of photosynthetic plankton increases dramatically. The timing and intensity of the spring bloom is dependent on underlying physical conditions that control ocean stratification and mixing. Although waves can be an important source of turbulent kinetic energy to the surface mixed layer, they have seldom been considered explicitly in studies of bloom formation. Here, we investigate the role of surface waves in bloom formation using a combination of satellite observations and numerical models. Satellite observations show a positive correlation between wave activity and chlorophyll concentration in the Northwest European shelf (May-September). In the deeper Northeast Atlantic, increased wave activity correlates with lower chlorophyll during periods of high phytoplankton activity (March-May) and higher chlorophyll when activity is low (below $54°$N, July-September). We use a first-of-its-kind, km-scale, two-way coupled model system to investigate both the relationship between wave mixing and bloom formation, and the sensitivity of model results to the method by which wave mixing is ~~parameterised~~parametrised. In deep regions, during the spring bloom, a wave mixing event is likely to mix surface chlorophyll to deeper layers, away from light. In contrast, when ~~and where~~ phytoplankton activity is low in deep regions, wave mixing can entrain nutrients, fueling the growth of nutrient starved phytoplankton near the surface. In June to October, in shallow but weakly stratified regions of the shelf, surface chlorophyll tends to be elevated following a wave mixing event, which can bring to the surface both phytoplankton and nutrients from deeper layers~~and nutrients~~. When contrasted with ~~ocean only~~ ocean-only runs, the two way-coupled ocean-wave model tends to produce greater vertical mixing and a delay in bloom onset. These results indicate bloom dynamics are sensitive to the way in which waves are modelled, and that the role of waves in bloom formation should be considered in future studies.

1 Introduction

The spring bloom is a defining feature of annual marine primary production in temperate waters of the Northeast Atlantic and adjoining shelf seas. It is characterised by a rapid increase in the abundance of phytoplankton - photosynthetic microorganisms

that are the ocean's dominant primary producers. Following winter, the spring bloom provides the first major influx of food for the rest of the marine food web, and many organisms have adapted their development to take advantage of the increased food supply (Cushing, 1990; Ji et al., 2010; Cyr et al., 2024). The spring bloom is tightly linked to changes in the physical environment at the end of winter; a link first identified by G. A. Riley in the early 1940s (Riley, 1942). However, the exact trigger for the spring bloom is still debated. Sverdrup proposed the Critical Depth Hypothesis, which states that the spring bloom occurs when the thermocline rises above a critical depth (Sverdrup, 1953). Sverdrup's critical depth is the maximum depth a phytoplankton cell can be mixed down to while , on average, still receiving enough light to offset losses associated with respiration and other processes. When the thermocline is above the critical depth, phytoplankton cells are trapped in well-lit, nutrient-replete waters near the surface where conditions are favourable for growth and reproduction.

Another proposed explanation for the timing of bloom formation is the Critical Mixing Hypothesis, which states that a bloom can form in a mixed water column if the rate of mixing is low enough for phytoplankton near the surface to achieve net positive growth (Huisman et al., 1999). This mechanism was explored by Taylor and Ferrari (2011) using high resolution, three-dimensional ocean models, with a reduction in net cooling at the end of winter identified as a key trigger. Biological controls on bloom formation have also been proposed, including the Dilution-Recoupling hypothesis, which focuses on the balance between phytoplankton growth and grazing pressure through winter and into spring (Behrenfeld, 2010). Although the exact mechanism controlling bloom formation is still debated, a recent study using autonomous underwater gliders lent most support to Sverdrup's Critical Depth Hypothesis based on the depth of active mixing (Rumyantseva et al., 2019).

In tidally active areas on the continental shelf, stratification and bloom formation are also dependent on the water depth and the degree of mixing in the bottom boundary layer. Shallow regions of the Northwest European Shelf (NWES), including areas in the English Channel and the southern North Sea, remain permanently mixed year round (van Leeuwen et al., 2015). Other areas may be intermittently stratified, depending on prevailing tidal and atmospheric conditions. The bloom itself can be interrupted by an increase in bottom mixing associated with the spring-neap tidal cycle, or the passage of a storm, leading to an apparent double bloom (Sharples et al., 2006).

Once established in deeper , seasonally stratified waters, stratification can be difficult to break down, requiring extreme atmospheric conditions, such as those associated with the passage of a hurricane or typhoon, to fully mix the water column (Shi and Wang, 2007; Babin et al., 2004; Sharples et al., 2001). Such events can trigger a new bloom in their wake, fueled fuelled by a fresh influx of nutrients that have been mixed up from below the nutricline. In the absence of an extreme mixing event, the bloom will often peak before reducing in intensity as the supply of nutrients is exhausted and top-down pressures from grazing and viral lysis take hold (Simpson and Sharples, 2012). Near to the nutricline, given sufficient light, it is common for a sub-surface chlorophyll maximum to form in the summer. As stratification begins to break down at the end of winter summer, an autumnal bloom can sometimes be observed.

While the spring bloom is an annual event, its timing, duration and intensity exhibit significant inter-annual variability. Using models driven at the surface by winds and changes in the net heat flux, Waniek (2003) showed the spring-time shallowing of the mixed layer can be interrupted by mixing events caused by weather systems whose frequency and intensity vary from year

60 to year, leading to ~~interannual~~ inter-annual variability in bloom dynamics. This is a result that is embedded in contemporary coupled hydrodynamic-biogeochemical models, which are typically forced at the surface by a set of common variables, including wind, surface pressure, surface temperature, net ~~shortwave~~ short-wave radiation and fresh water fluxes.

One aspect that isn't typically considered ~~explicitly~~ in studies of bloom dynamics is the impact of surface waves on turbulent

65 mixing~~.~~, despite evidence that bloom timing can be closely coupled to meteorological indices (Powley et al., 2020). The impact of waves on the ocean may either be parametrised in an ocean only model, or modelled explicitly using a combination of ocean and wave models in a two-way coupled configuration. In ocean only models, the input of turbulent kinetic energy at the ocean surface often follows the assumption that wind and waves are in equilibrium with each other, which is only valid under certain wind regimes and in the deep open-ocean, far from coastlines (Cavaleri et al., 2012). Surface waves also induce Lagrangian

70 drift in their direction of propagation, known as Stokes drift (Phillips, 1977; Stokes, 1847) – a process not usually taken into account in stand-alone ocean models. Wave breaking terms and their impact on the vertical eddy diffusivity are sometimes considered, but often include assumptions relating to the water-side momentum flux (Craig and Banner, 1994) and surface roughness calculations; with the wave-age and significant wave height estimated as functions of the water-side friction velocity (Rascle et al., 2008).

75 Traditionally, models for different components of the Earth system - the atmosphere, land, ocean and ocean waves - have been run independently. However, with improvements in computing power, studies using two-way coupled model configurations are becoming increasingly common (Berthou et al., 2025b). ~~Wave breaking induces turbulent mixing which helps to stir the ocean's surface, with a direct feedback on atmosphere-ocean exchange.~~ Recent studies have shown the benefits of coupling a wave model to an ocean model ~~in terms of marine~~ to derive these terms more accurately in high resolution

80 configurations (Lewis et al., 2019; Bruciaferri et al., 2021; Valiente et al., 2021). This has led to improvements in the forecasting of extreme wave heights and surges, ocean mixing (Lewis et al., 2019)~~;~~, and surface currents (Bruciaferri et al., 2021). Replacing the ~~implicit~~ parametrised calculation of wave-induced mixing in the ocean by ~~explicit coupling to a wave model induces~~ an explicit wave model through coupling can have variable effects depending on the wave momentum calculation in the stand-alone ocean model set-up: in the case of Lewis et al. (2019), which used a similar set up to our study, two-way

85 coupling tended to induce enhanced vertical mixing~~and better represents Stokes drift (Bruciaferri et al., 2021). This leads~~, leading to a deeper summer mixed layer, resulting in a relative cooling of surface and upper ocean temperatures during periods of stratification~~(Lewis et al., 2019). The~~. In the case of Alari et al. (2016); Øyvind Breivik et al. (2015), the impacts of wave coupling on the ocean ~~are generally weaker in shallow on-shelf areas, which is likely a result of them being mixed by tidal processes throughout the year (Lewis et al., 2019)~~tended to reduce summer mixing and generated enhanced upwelling in the

90 Baltic Sea due to the additional Stokes drift. This highlights the value of wave coupling, but also the need to modify turbulence

parametrisation schemes in ocean models to account for wave coupling (Couvelard et al., 2020).

~~Liu et al. (2025) observed a delay in~~ Wave-induced mixing has been observed to impact phytoplankton dynamics when included in coupled hydrodynamic-biogeochemical models, both by delaying the spring phytoplankton bloom ~~in the South China Sea when a parameterisation of wave induced mixing was added to a coupled hydrodynamic-biogeochemical model, suggesting a sensitivity to wave induced mixing~~ and enhancing chlorophyll-a levels at the surface and at depth (Liu et al., 2025; Tensubam et . In this study, we investigate the sensitivity of bloom timing and ecosystem processes ~~to wave coupling~~ across the NWES and the Northeast (NE) Atlantic by coupling a wave model to an ocean-biogeochemistry model. This region is located at the end of the northern and central branches of the North Atlantic storm track (Woollings et al., 2010), and is therefore subject to high wave activity in the winter, and episodic wave activity in summer. The NWES is also an extremely productive region, with a pronounced spring bloom evident over large areas of the shelf (Simpson and Sharples, 2012). Specifically, we address the following questions: (i) What is the relationship between wave activity and phytoplankton bloom phenology? (ii) How sensitive are model results to the ~~implicit~~ parametrised and explicit representation of wave mixing effects?

For ~~the~~ this study, we use the UK Met Office's operational ocean-wave coupled model system, which has been extended by coupling it to the European Regional Seas Ecosystem Model (ERSEM) (Butenschön et al., 2016). The new system allows for two-way ~~feedback~~ feedbacks between each model component to be represented, providing a more realistic representation of surface mixing and ecosystem responses. This representation contains several wave-induced processes that are absent from the non-coupled system. The study represents the first time a coupled ocean-wave-biogeochemistry model at km-scale resolution has been used to simulate ecosystem processes across the NWES and NE Atlantic. The modelling work is complemented by an analysis of both satellite and in situ observations.

The plan for the paper is as follows. In section ~~??~~2, we describe the study area and quantify relationships between satellite ocean colour and wave reanalysis data for recent decades. We then focus on the year 2018, when three named storms passed over the UK between the months of June and September, and examine the temporal evolution of phytoplankton abundance over the course of the year. In section ~~2~~3, we describe the modelling tools which we use to simulate the year 2018, showing the results of the modelling study in section 4. In section ~~4~~5, we use the models and observations to compare bloom phenology and ecosystem responses to summer wave activity, and investigate the impacts that wave coupling has on ocean physics and biogeochemistry. Finally, in section ~~5~~5.3, we bring the modelling and observation results together to propose mechanisms for the phytoplankton activity response to wave activity shown in section 2.
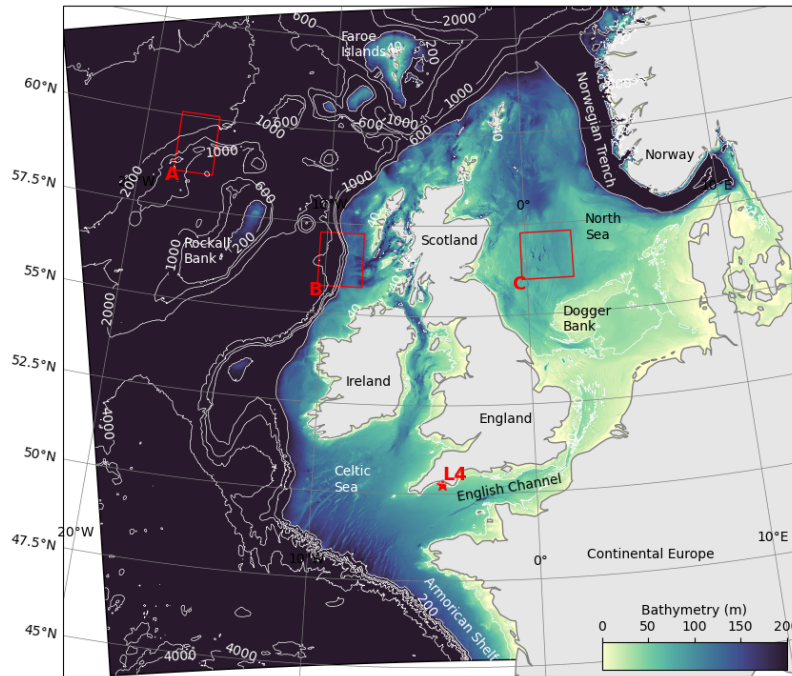
Figure 1. AMM15 model domain extent with bathymetry contours (m). Red boxes highlight representative analysis zones for off-shelf (A), shelf break (B) and on-shelf (C) areas. The L4 monitoring station is shown with a star.

2 The Northwest European Continental Shelf and North East Atlantic

2.1 Physical and hydrodynamic characteristics

The NWES is a broad temperate continental shelf on the eastern side of the North Atlantic Ocean (Fig. 1). The region is demar-
125 cated by the shelf break, which extends ~~northwestward~~ north-westward through the Bay of Biscay in the south, along the edge of the Amorican shelf and up and around the west coasts of Ireland and Scotland, then ~~northeastward~~ north-eastward toward the west coast of Norway. Topographic steering drives the northward flow of water parallel to the shelf slope, with more limited cross-slope transport driven by surface winds and meandering eddies. ~~Off shelf~~ Off-shelf, in the north of the region, the North Atlantic Current flows ~~northeastward~~ north-eastward between Iceland and Scotland. Water enters the North Sea in the north
130 through central and western regions of the northern North Sea, and in the south through the English Channel. The dominant outflow from the North Sea is via the Norwegian Coastal Current.

~~On shelf~~ On-shelf, dynamics are controlled by seasonal changes in solar irradiance and heating, atmospheric fluxes and wind forcing, tides, river inputs and exchanges with the open ocean. Large areas of the shelf are seasonally stratified, including
135 in the Celtic Sea, western reaches of the English Channel and the central North Sea. Shallower areas on the shelf may be

5

intermittently stratified or permanently mixed, with tidal mixing fronts separating stratified and well mixed areas. Nutrient concentrations are influenced by exchanges with the open ocean, atmospheric deposition and, particularly in coastal areas, river discharge. Bottom-up controls on the growth of phototrophic plankton include the availability of light and nutrients; and temperature. The spring bloom typically occurs from late March into April (Racault et al., 2012), and tends to start in the south of the domain before spreading northward. In coastal waters with high sediment loads, the growth of surface plankton can be light limited. In the summer, under stratified conditions, surface phytoplankton become nutrient limited.

2.2 Monthly wave energy relationship to observed chlorophyll concentration in climatology

To explore the potential impact of waves on bloom dynamics in the NE Atlantic and on the NWES, we examine satellite ocean colour and wave reanalysis data. We used chlorophyll-a from the Ocean Colour Climate Change Initiative (OC-CCI) dataset (Sathyendranath et al., 2019, 2023) and wave energy from the Met Office regional wave hindcast from WAVEWATCH III (Saulter, 2024) to calculate ~~interannual~~ inter-annual correlations between bimonthly-mean chlorophyll concentrations and wave energy from 1998 to 2020. To achieve this, the temporal mean was calculated across pairs of months for each year from March to November, when the majority of primary production occurs. Wave energy and chlorophyll data were then normalised at each spatial pixel and the Pearson correlation coefficient calculated between them, with significance tested using a two-sided p-value for the correlation being different to zero (Virtanen et al., 2020).

The results show a strong negative correlation between wave energy and chlorophyll concentration ~~off shelf~~ off-shelf and near the shelf break in March-May, and a strong positive correlation on-shelf from June to October (Figure 2). This suggests that stronger wave activity in the open ocean when phytoplankton are blooming in March-May leads to a reduction in surface chlorophyll, whilst the reverse is true on-shelf later in the year. ~~Off shelf~~ Off-shelf, the response to enhanced wave activity appears positive in the ~~southwest~~ south-west of the domain from June to September. In the ~~northwest~~ north-west of the domain, the open-ocean response is confined to close to the shelf break ~~, and~~ and, where significant, is generally negative, except in August-September. Wave energy is likely not the sole causal factor in this correlation: increased storminess will also decrease available sunlight.

2.3 Wave activity and chlorophyll concentration in 2018

The year 2018 has been selected for this study as there was a cooler ocean surface in March-April, when the spring bloom typically occurs, and enhanced wave activity compared to climatological conditions (Fig 3). Later in the year, two marine heatwaves (MHW) developed. The first was in late May to mid-June and the second in July. The first was terminated by storm Hector, which passed over the UK between 13th and 14th June ~~2018. Storm Hector brought heavy rain and winds to~~ 2018, particularly impacting the North of the UK and Ireland. ~~In Northern Ireland, maximum gust speeds in excess of were recorded.~~ The second heatwave was terminated by an unnamed storm which passed over the UK on 29th July. Storm Ali and Bronagh
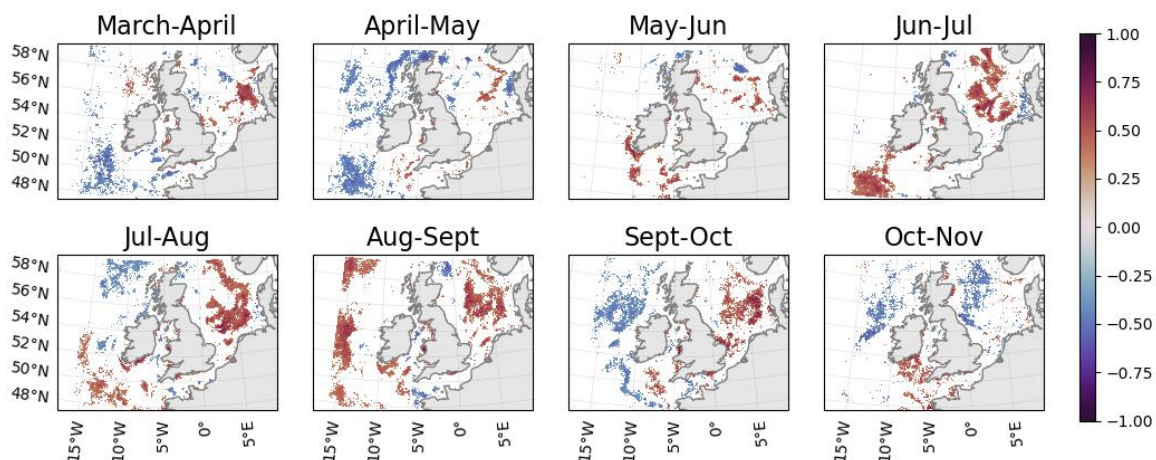
Figure 2. Correlation between mean wave energy and mean chlorophyll concentration from 1998 to 2020 for different pairs of months. Only regions where the correlation coefficient is significant (p<0.1) are coloured. Wave data is from a WAVEWATCH III reanalysis (Saulter, 2024) and chlorophyll satellite data is from OC-CCI (Sathyendranath et al., 2019, 2023).

passed over the UK in succession between 18th and 21st September.

170   ~~We used the approach of Jardine et al. (2022) to determine the timing of bloom onset. In this approach, bloom onset is defined as the start of exponential growth in the concentration of chlorophyll, which is used as a proxy for phytoplankton biomass. This is defined to be the time when the change in the concentration of chlorophyll exceeds consistently for 5 consecutive days, and is referred to as the date of exponential onset. This approach performs best with full temporal data coverage, ideally suited to evaluating model data. For satellite data with gaps in coverage the algorithm occasionally fails to identify the bloom, however~~

175   ~~for consistency we use the same approach for satellite and model data.~~

~~In 2018, phytoplankton bloom onset happened around mid-April in the south of the domain and drifted into May in the North and West, with large spatial variability (Figure **??**). On the shelf, bloom onset also generally occurred in April, although the bloom began later on the northern shelf break and parts of the Channel and Celtic Sea.~~

~~Date of onset of exponential phytoplankton growth in spring 2018 satellite data from OC-CCI (Sathyendranath et al., 2019, 2023)~~

180   ~~. Bloom onset calculated using the method from Jardine et al. (2022), where bloom onset is defined to occur when phytoplankton biomass increases by consistently for 5 consecutive days.~~

Late summer storms can either suppress or enhance chlorophyll, depending on timing and area (Fig. 4). In June, as a result of storm Hector, the concentration of chlorophyll was reduced in northern off-shelf areas, which were in bloom state, whereas chlorophyll increased on the western part of the shelf in regions which were past their bloom state. Particularly strong increases

185   are noticeable in the Celtic Sea, Irish Sea, and Southern North Sea. Following the July storm, chlorophyll concentration was low ~~off shelf~~ off-shelf and the storm had a minimal impact. In contrast, the concentration increased in coastal areas of the
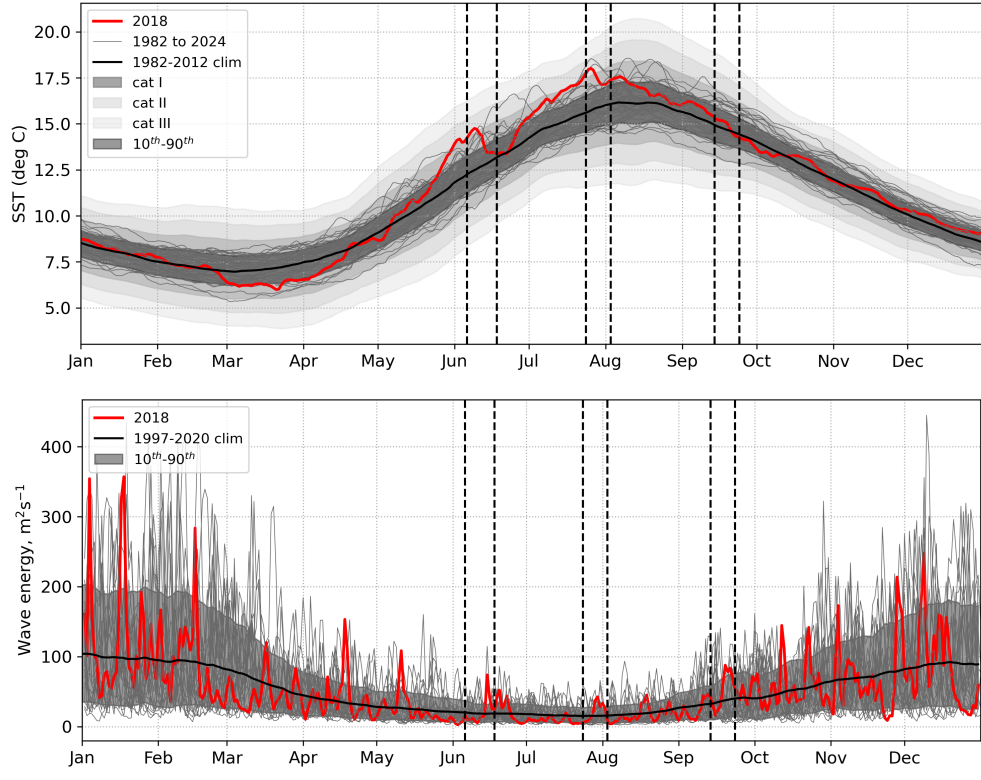
Figure 3. Top - Operational Sea Surface Temperature and Ice Analysis (OSTIA) SSTs for 1982–2022, mean climatology for the time period used to define marine heatwave thresholds (1982–2012) in bold, 10th–90th ~~centiles~~ percentiles (anomalies smoothed with 31-day moving average), Shading: Category I, Category II, Category III marine heatwaves using Hobday et al. (2018) averaged over the NWS. Bottom - Wave energy from Met Office wave regional reanalysis (Saulter, 2024) for 1997–2020. Yearly data shown with grey lines, mean climatology from 1997–2020 in black, 2018 in red. Grey shading between 10th–90th ~~centiles~~percentiles. Mean and ~~centiles~~ percentiles smoothed with 31-day moving average. Wave energy averaged over the NWS (NWS=blue+purple regions in Fig. 1). Vertical dashed lines indicate three key 2018 storm periods.
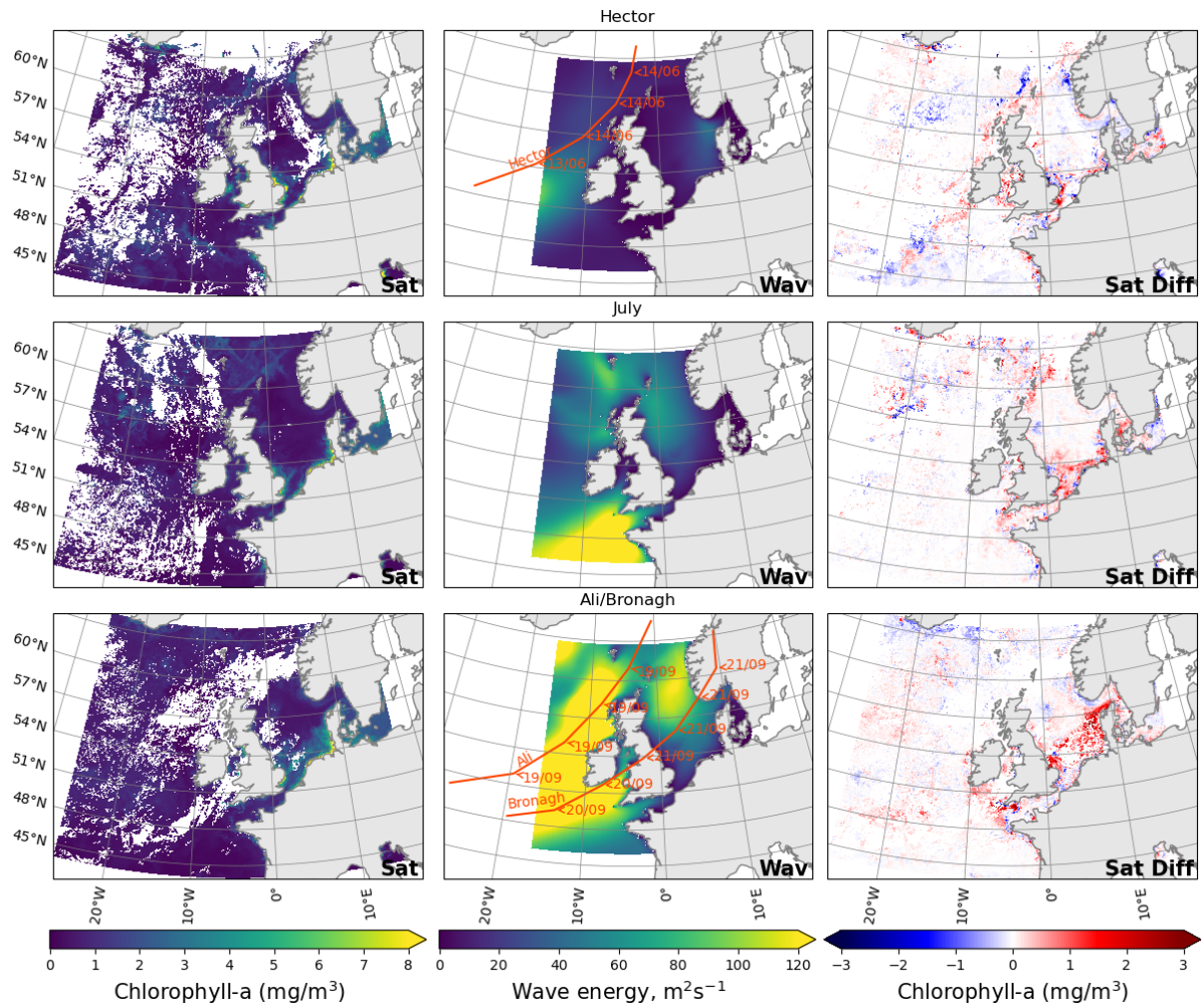
Figure 4. Mean chlorophyll from satellite in the five days before the storm (left), wave activity on the day of the storm from the Met Office wave regional reanalysis (Saulter, 2024) (middle) and difference in the mean satellite chlorophyll five days after and before (right) storm Hector (top), July storm (middle) and storms Ali and Bronagh (bottom). The start of the five days before and the end of the five days after the storms are highlighted in Figure 3 as vertical bars.
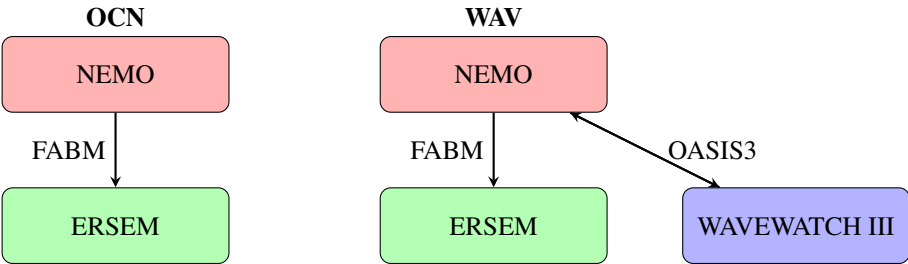
shelf. In September, northern areas tended to see a decrease in chlorophyll from storms Ali and Bronagh, whilst southern and on-shelf areas saw a strong increase.

190   The observations confirm 2018 to be an interesting year to study the relationship between wave activity and the concentration of chlorophyll~~and suggest that waves played a role in controlling chlorophyll concentrations in that year~~. Indeed, some years have uninterrupted summer stratification (e.g. 2017, used in Lewis et al. (2019)): we choose a year in which wave activity was enhanced in spring and had intense summer wave activity events able to disrupt the ocean stratification. In the remainder of the

article, we focus on how intense periods of wave activity affected the concentration of chlorophyll, and how explicitly coupling
an ocean model to a wave model impacts model results.

3   Model Framework

The impact of ocean-wave coupling on biogeochemistry is assessed through a twin experiment. Experiments are conducted
with (WAV) and without (OCN) the coupled wave model in order to examine the biogeochemical response, as shown in Scheme
1.

Scheme 1: Twin experiment configurations

3.1   Hydrodynamic Model

Both simulations have been performed using the Nucleus for European ~~Modeling~~ Modelling of the Ocean (NEMO) model
(Madec et al., 1998), adapted for simulating shelf sea dynamics (O'Dea et al., 2012). For this study, we use NEMO v4.04.
The model domain is the high-resolution $1.5\,\text{km}$ Atlantic Margin Model (AMM15) configuration (Fig. 1), which is used for
operational forecasting by the UK ~~MetOffice~~ Met Office (Tonani et al., 2019). In contrast to the more commonly used $7\,\text{km}$
configuration for the same region (AMM7), the high resolution domain ~~enables smaller scale features~~ better resolves smaller
scale processes such as eddies~~and internal tides to be better represented (Graham et al., 2018a, b)~~, fronts and internal waves
(Graham et al., 2018a, b), all of which can influence wave activity.

Initial fields for the simulations were provided by a previous ocean-wave experiment (Lewis et al., 2019), with lateral
boundary ~~forcings~~ forcing from global ocean models. Meteorological forcing is provided at 3-hourly intervals from the UK
Met Office global Unified Model analysis, at a ~~25km~~ 25 km resolution. There is no live coupling from sea-surface back to the
atmosphere.

For the ~~OCN simulation, the vertical eddy viscosity is computed using the two-equation GLS turbulent closure model. In
the absence of a two-way coupled wave model, the impact of waves on the ocean is parameterised~~ uncoupled OCN simulation

a limited, parametrised version of waves are included in the following way (see Reffray et al. (2015) for ~~the~~ full details about
the NEMO implementation):

1. ~~surface enhanced mixing due to wave-breaking according to Craig and Banner (1994) scheme;~~

2. ~~sea surface roughness~~ Sea surface roughness is approximated as a function of the estimated significant wave height ~~,~~ ~~approximated~~ based on wind speed, as proposed by Rascle et al. (2008)~~. Additionally, it is assumed that the water-side~~;

3. Water-side momentum flux (i.e., the wind stress τ_{atm}) is completely transferred into the ocean~~.~~;

4. Vertical eddy viscosity is computed using the two-equation GLS turbulent closure model, taking into account:

    (a) Parametrised surface enhanced mixing due to wave-breaking ((Craig and Banner, 1994)), a function of water-side friction velocity depending on wind stress;

    (b) Sea surface roughness z_0, estimated as above.

3.2 Wave Model

~~The wave component of the NWS prediction system is AMM15-wave,~~ To better resolve waves effects, NEMO is coupled to a
regional implementation of the WAVEWATCH III spectral wave model version 4.18 (Tolman, 2014) as detailed in Saulter et al.
(2017). The domain~~of,~~ AMM15-wave, covers the same ~~area~~ extent as the AMM15 NEMO model but uses a Spherical Multiple
Cell discretization scheme (Li, 2012) configured to have a variable horizontal resolution ranging from $3\,\mathrm{km}$ across much of
the domain down to $1.5\,\mathrm{km}$ near the coast or where the average depth is shallower than $40\,\mathrm{m}$. Wave growth and dissipation
terms are ~~parameterized~~ parametrised following Filipot et al. (2010) while ~~nonlinear~~ non-linear wave-wave interactions use the
Discrete Interaction Approximation (DIA) package according to Hasselmann et al. (1985).

3.3 ~~Wave-Ocean coupled model~~

Two-way coupling utilises the OASIS3-MCT coupler (Valcke et al., 2015). NEMO shares water levels and currents with the
spectral wave model. In turn, WAVEWATCH III injects Stokes drift, significant wave height and water-side momentum flux
into the hydrodynamic model. The coupling frequency is hourly.

~~In this system, the~~ By explicitly coupling WAVEWATCHIII to NEMO, as in the WAV experiment, the ocean momentum
budget equation ~~solved by the ocean model~~ is modified to include three wave feedbacks as described in Bruciaferri et al. (2021).
~~The first is the~~

1. Surface waves induce a mean Lagrangian drift in their direction of propagation known as Stokes drift (e.g., Phillips (1977); Stokes (18
). When the wave-induced drift interacts with the planetary vorticity, an additional force named the Coriolis-Stokes force
   (CSF) ~~, an interaction between the Stokes drift in the direction of propagation of waves and the Coriolis force. The~~

second is a wave modified water-side momentum flux: the wavefield is not always appears in the wave-averaged Eulerian momentum equation (Hasselmann, 1970). Stokes Drift at the surface is computed by the wave model and exchanged with the ocean model together with the significant wave height and the mean wave period, so that the ocean model can calculate the depth-varying 3D Stokes drift according to Øyvind Breivik et al. (2016).

2. Wind blowing on the sea surface generates both ocean waves and currents. As a result, sheared ocean currents are directly forced by the total wind stress, τ_{atm}, only in the case of fully developed wind-waves (Jr. and Moskowitz, 1964) . Most of the time, the wave field is far from being in equilibrium with the local wind as assumed in the standalone ocean model (especially in coastal areas like the NWS). The , and waves are either growing, with a net influx of momentum into the wavefield wave field, or decaying, with intensified wave-breaking and a net outflux of momentum from waves into the ocean (e.g., Komen et al. (1994)). Lastly, a sea-state dependent sea surface roughness (calculated from the significant wave height), is taken into account in the calculation of the vertical eddy viscosity , as explained in Section 3.1. Note the wave-breaking term is still calculated by the ocean only system, but will be modulated by the change in Komen et al. (1994)). Thus, when surface waves are considered the water-side momentum described above. momentum flux τ_{ocn} (i.e., the stress that effectively forces the ocean at the surface) is given by:

$$\tau_{ocn} = \tau_{atm} - \tau_{atw} + \tau_{woc} \tag{1}$$

where τ_{atw} is the momentum flux absorbed by the waves (aka the wave-supported stress) and τ_{woc} is the momentum flux from the wave field to the mean flow. In the wave-ocean coupled model, τ_{woc} is computed by the wave model and directly passed to the ocean model.

3. Vertical eddy viscosity is still computed using the two-equation GLS turbulent closure model (Reffray et al. (2015)), with the following changes:

   (a) Surface enhanced mixing now dependent on τ_{woc} instead of τ_{atm}.

   (b) Sea surface roughness as a function of the significant wave height provided by the wave model.

Due to limitations of the GLS turbulence scheme there are some processes that WAVEWATCH III resolves which are not currently configured to directly influence the ocean model through coupling. These include the effect of wave breaking on the surface turbulent kinetic energy budget (following Craig and Banner (1994)) and explicit treatment of Langmuir turbulence, (e.g. through use of a vortex-force formulation Uchiyama et al. (2010) or of ocean bed stress linked with wave/current interactions Zhang et al. (2022)).

In this study the inclusion of wave feedback in NEMO through WAVEWATCH III in the WAV simulation is referred to as *explicit* wave coupling, whilst the standard approach of NEMO in the OCN simulation is referred to as *parametrised* waves.

3.3 Biogeochemical Model

280 For this study, we use the European Regional Sea Ecosystem Model (ERSEM) for simulating ocean biogeochemistry and phytoplankton bloom dynamics (Butenschön et al., 2016). ERSEM has been coupled to NEMO using the Framework for Aquatic Biogeochemical Models (FABM) (Bruggeman and Bolding, 2014). FABM facilitates passing data between biogeochemical and hydrodynamic models. Here, the coupling is one way, and the biogeochemical model does not feedback onto ocean physics. Whilst ERSEM is not directly coupled to the wave model, biogeochemical processes are influenced by changes 285 in ocean currents and mixing that are caused by the wave model.

Biogeochemistry Initial & Boundary Conditions ~~To the authors' knowledge, at the time of simulation this~~ This is the first instance of ERSEM being used with the NEMO AMM15 domain. Initial values are interpolated from a reanalysis run performed on the coarser AMM7 domain for November 2016. Since the north-west corner of the AMM15 region extends beyond 290 the bounds of the AMM7 domain, extrapolation is performed using a simple nearest neighbour algorithm. Before performing the 2018 experiment, a fourteen month ocean-biogeochemistry only simulation starting on 1st November 2016 is used to 'spin-up' the biogeochemical initial conditions and negate any impact of extrapolation.

A constant supply of non-depleting nutrients at the boundary can lead to spurious phytoplankton blooms and other unre- 295 alistic responses. This is mitigated by enforcing a ~~low, constant value~~ constant value matching the near-zero winter values at the boundary for most of the previously unconstrained tracer fields ~~(Polton et al., 2023)~~ following the guidance in Polton et al. (2023). Biogeochemical surface boundary conditions include nitrogen deposition from the atmosphere and light attenuation due to detritus and yellow matter (the Gelbstoff absorption coefficient). Nitrogen deposition data is available at monthly resolution using models run by the European Monitoring and Evaluation Programme (EMEP) (Simpson et al., 2012), which are then 300 converted into fluxes for both oxidised and reduced components. The Gelbstoff absorption coefficient is produced using data from OC-CCI (Sathyendranath et al., 2019), for a multitude of wavelengths that are integrated into a single broadband field.

River input data is an updated version of the files used in the CMEMS ~~northwest~~ north-west European shelf reanalysis from Lenhart et al. (2010). A climatology from the Global River Discharge Database (Vörösmarty et al., 2000) and data from the 305 Centre for Ecology and Hydrology (Young and Holt, 2007) have been used to provide time varying daily river discharge, nutrient loads (nitrate, ammonia, phosphate and silicate), total alkalinity, dissolved oxygen and dissolved inorganic carbon.

4 Modelling Results

4.1 Validation

In Lewis et al. (2019); Graham et al. (2018a, b), a detailed validation of the physical ocean and wave models has been performed, demonstrating good performance of stand-alone models and improvements to significant wave height and total water level extremes when coupling ocean and waves (Lewis et al., 2019). For biogeochemistry, while there have been several modelling studies using ERSEM on the coarser AMM7 domain (e.g. Jardine et al., 2022; Powley et al., 2024), this experiment is the first simulation of ERSEM biogeochemistry on the $1.5\,\mathrm{km}$ regional domain.

Profiles of temperature extracted from the EN4 Met Office Hadley Centre Observation Dataset (Good et al., 2013) were compared to predicted profiles of temperature from both the OCN and WAV models for March to June (Fig. 5) in off-shelf areas deeper than $200\,\mathrm{m}$. Both models show a persistent warm bias off-shelf, which is due to the combination of surface forcing that itself has a warm bias and model drift before the start of our 2018 simulations. The coupling of waves results in a marginal improvement during spring when the water column is well mixed, but as it stratifies in June the impact of waves increases leading to a reduction in the overall bias.

The warm bias for temperature is also present when compared to satellite surface fields from the Operational Sea Surface Temperature and Ice Analysis (OSTIA) (Fig. 6), with a persistent positive bias across most of the domain. The warm bias results in a combination of higher phytoplankton growth rate and a higher rate of mineralisation of summer nutrients. Therefore it is no surprise to also see a positive bias across most of the off-shelf domain for chlorophyll compared with OC-CCI surface satellite measurements for 2018 (Fig. 6). Unlike temperature, on-shelf and coastal areas have a negative bias with the greatest values in areas close to river mouths. In part, the bias is a result of using climatological river input data, which prevents the model from capturing inter-annual variability in river inputs and their impact on ecosystem dynamics.

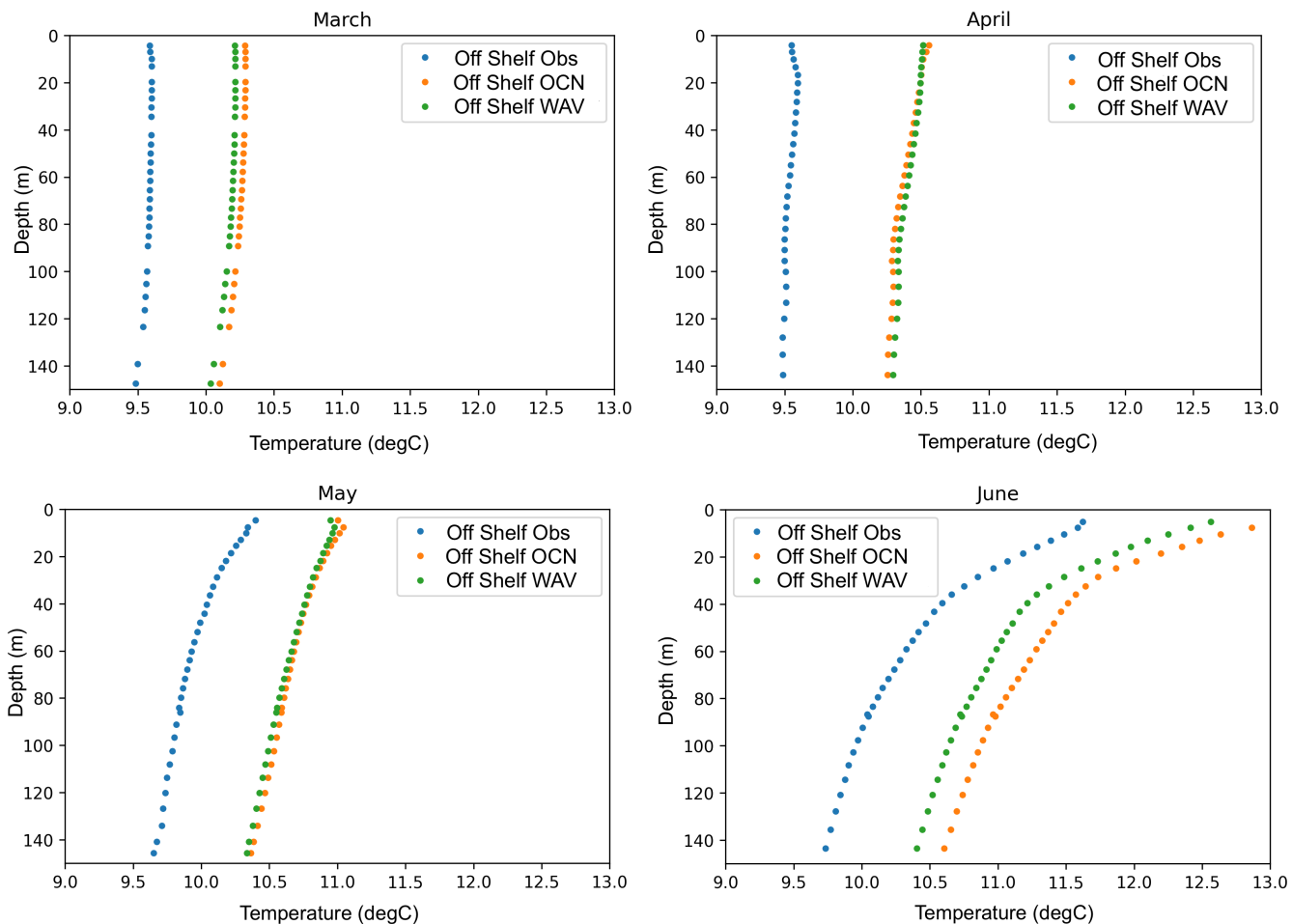| Variable	Observed Mean	Model Mean	Bias	Spatial Correlation	Temporal Correlation
Temperature ($^\circ C$)	11.69	12.54 (12.37)	0.85 (0.68)	96.7% (97.2%)	98.0% (98.3%)
chlorophyll (mg/m^3)	0.83	1.08 (1.08)	0.25 (0.25)	-0.14% (-0.13%)	48.9%

Figure 5. Potential temperature profiles within the off-shelf region, averaged over all observed profiles in the EN4 database that are located within $1.5 \, \text{km}$ of a model grid cell for March, April, May and June (blue), along with the corresponding simulated profiles at the same point and time for the OCN (orange) and WAV (green) simulations.
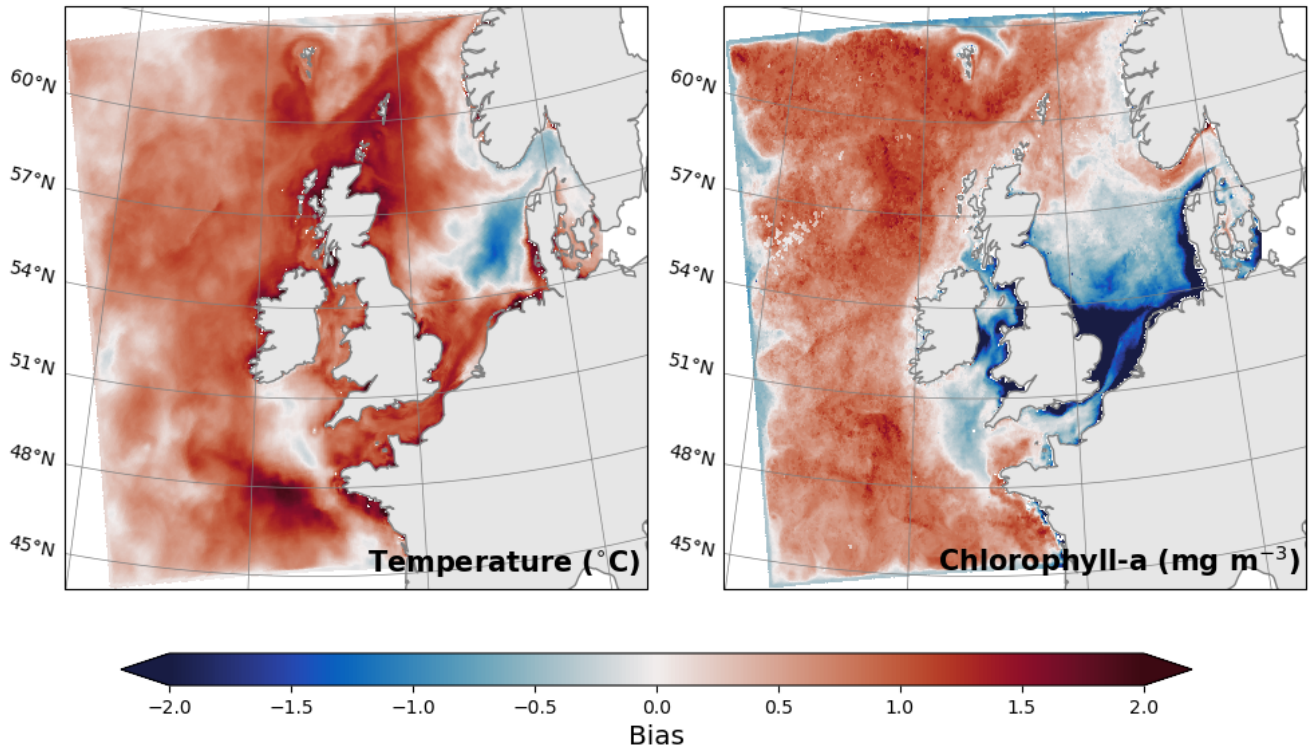
Figure 6. Annual mean bias at the surface between the ocean-only model and (left) satellite temperature from OSTIA, or (right) chlorophyll from OC-CCI.

~~(47.2%)Summary statistics for key variables at the surface matched against satellite observations for temperature (OSTIA) and chlorophyll (OC-CCI). Results from the simulation with wave coupling are provided in parentheses.~~

For in situ observations of biogeochemical variables, we use data from the long-term monitoring site Station L4 (McEvoy et al., 2023), which is located on the western edge of the English channel (Fig. 1). ~~The area is influenced by freshwater inputs~~

345   ~~from the river Tamar. While the use of climatological river forcing datameans the model will fail to reproduce inter-annual~~ ~~variability in river inputs, the data provides an opportunity to investigate the relative impact of wave coupling~~This site contains valuable observational data, albeit in a region where wave activity does not have a significant impact. Fig. 7 shows a comparison of the two simulations with observations for surface temperature, salinity and chlorophyll-*a* from Station L4. Also plotted are Net Primary Production (NPP) from both model runs and Significant Wave Height from the WAV simulation. Temperature

350   is consistent between the models~~and correlates well to the observations~~, with the warm bias vs observations evident over the winter months ~~and the~~ (Fig. 7a). The effect of the marine heatwaves is clearly visible in the observations~~(Fig. 7a).~~, whilst the response in the models is more muted. In winter months, the WAV model is more saline at the surface (Fig. 7b), indicating greater mixing of buoyant, freshwater inputs from the river with more saline waters. These periods typically correspond to times
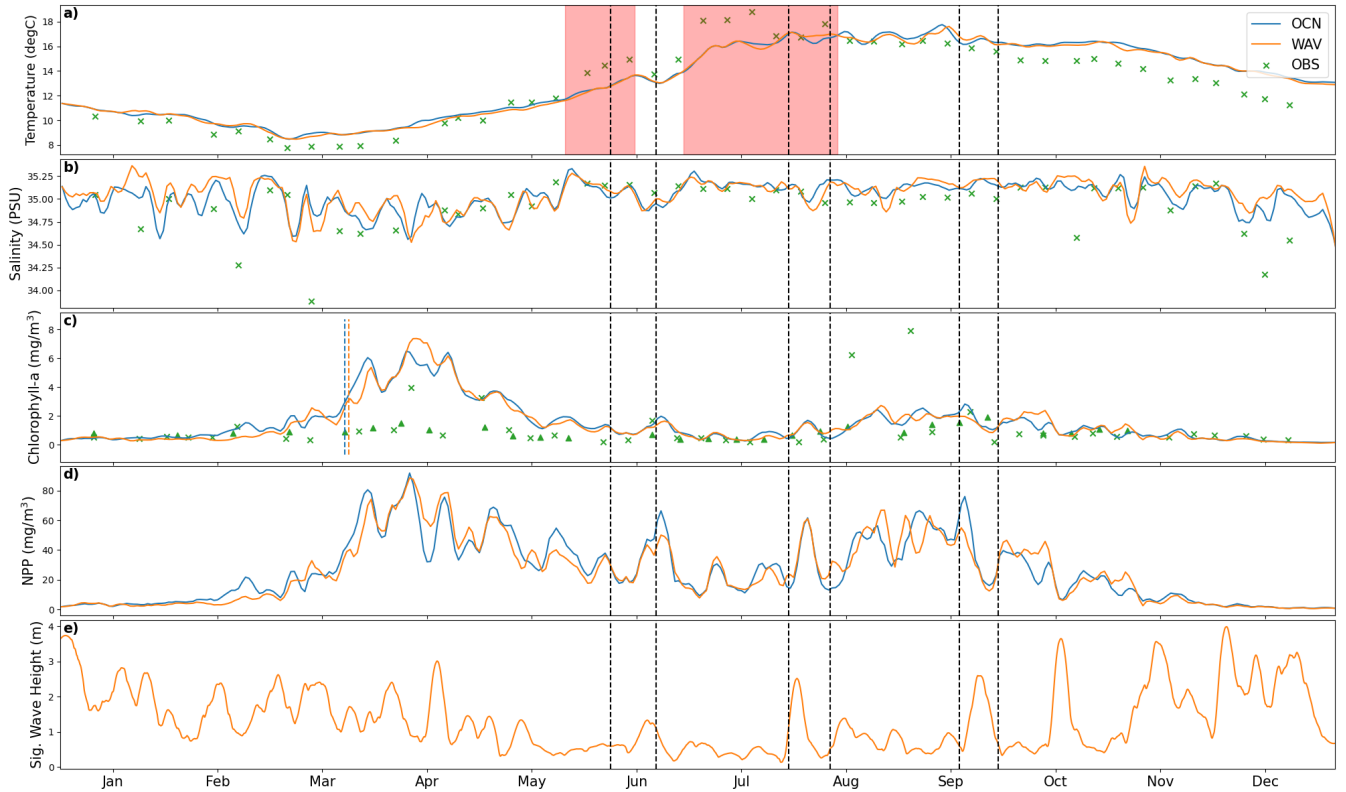
16

Figure 7. Surface comparison of modelled and observed biogeochemical variables at the L4 station (Fig. 1). Observations are from the Western Channel Observatory (McEvoy et al., 2023), with the addition of OC-CCI satellite chlorophyll (triangles). Red zones indicate ocean heat waves, black vertical dashed lines denote the storm times and the blue/orange vertical lines are the estimated bloom onset time.

of higher wave activity (Fig. 7e). Low salinity events seen in the observations are missed due to the use of climatological rivers missing high rainfall events. The inclusion of waves has only a minor impact on the spring bloom at this location (Fig. 7c), with slower initial growth and a slightly delayed peak. ~~Here, the model predicts the bloom a few weeks before the observations suggest it is occurring, with a late bloom seen in the area in the satellite data (Fig. ??). The trends identified in chlorophyll are also evident when examining net primary production (Fig. 7d). The same pattern of a short period of lower values in the WAV run followed by a longer period of higher values is also evident in September at the time of the autumn bloom~~ For most of the year the models over predict the chlorophyll, consistent with the findings in Fig. 6. The models also miss the late bloom in August that appears in-situ observations, although there is no evidence in the satellite measurements of a bloom at this time.

4.2 ~~Bloom phenology~~

17

Whilst the use of biased surface forcing prohibits an in depth comparison between the model and observations, the use of a twin experiment enables us to evaluate the impact of wave processes through explicit coupling from a mechanistic perspective.

Coupling with waves delays the bloom onset across most of the model domain (Fig. 10). On-shelf, the response to wave coupling is minimal as the shallow waters are already well mixed by tidal processes, whereas

4.2 Phytoplankton changes with wave coupling

Fig. 8 shows the simulated chlorophyll concentration throughout the year for a transect in the off-shelf bloom onset is typically 1-2 weeks later with larger delays in the south. In addition to delaying bloom onset, the yearly total of chlorophyll averaged over the euphotic depth is up to higher in the high-productivity region along the northern reaches of the shelf break and also in some deeper waters (Fig. 10).

Date of onset of exponential growth (top) and total NPP over the year averaged to the euphotic depth (bottom) for OCN (left), WAV (middle) and the difference; WAV minus OCN (right).

Relative to the date of bloom onset derived from satellite observationsof sea surface chlorophyll (Fig. ??), the date of bloom onset in the model runs is around 1 month later. Delays in bloom onset relative to observations have been observed in past NEMO-ERSEM simulations (Skákala et al., 2020), and, in part, stem from the parameterization of photosynthesis, phytoplankton growth and grazing effects. The biological model is also influenced by biases in the physical model, including temperature, which directly impacts biological rates as well as the timing of stratification; and the ability to accurately represent optically active components, such as coloured dissolved organic matter (cDOM) and suspended particulate matter (SPM), which impact light attenuation. Nevertheless, spatial variability is captured by the model, such as pockets of very late bloom over the shelf; and the later bloom onset along the shelf break north of Scotland and in the open ocean around . The south-north gradient is also evident in both the model runs and observations, although it is more pronounced in the model.

4.2.1 Response of phytoplankton to summer wave activity

Figure 14 shows the phytoplankton response to the three summer storms. The response can be contrasted with the observed response, as inferred from satellite observations (Fig 4). It is necessary to analyse the response in the context of the later, simulated bloom onset date. In June, this results in chlorophyll concentrations that are generally higher in the model relative to observations. As a result, in absolute terms, Storm Hector has a larger impact on sea surface chlorophyll concentrations than it does in the observations. The spatial pattern of the response to the storm is relatively similar between the model and the observations, with a suppression of phytoplankton activity off-shelf and increased activity on-shelf. For the July storm, the model represents well the increase in the concentration of chlorophyll on the western and northern edges of the North Sea. However, there is little effect of the storm off-shelf in the observations, whereas the model shows an increase in the concentration of chlorophyll. For storms Ali and Bronagh, the north-south gradient in the response in the North Sea is well captured by the model, though it is not as intense.

~~Coupling with waves deteriorates the model response to the June storm due to the bloom occurring later, which results in a phytoplankton reduction rather than increase west of Ireland. Similarly, in September, the wave model reduces the areas where chlorophyll concentrations increase in the southwest of the domain, which is less in line with a widespread off-shelf increase in the observations.~~

~~Mean chlorophyll in the five days before the storm from the ocean-biogeochemistry model (left), the difference between the mean of the five days after the storm and the mean of the five days before the storm from the ocean-biogeochemistry model (middle) and the ocean-wave-biogeochemistry model (right), for storm Hector (top), July storm (middle) and storms Ali and Bronagh (bottom). The start of the five days before and the end of the five days after the storms are highlighted in Figure 3 as vertical bars.~~

5 ~~Wave Coupling Impacts~~

~~In this section, we carry out a more detailed analysis of the impact of wave coupling on biogeochemistry by assessing the differences between the two simulations. This allows us to isolate the impact of wave coupling, while accounting for biases in the models relative to observations.~~ region running N-S. Chlorophyll fields are averaged ~~over~~ down to the euphotic zone, ~~to~~ the depth at which light is $1\,\%$ of its surface value, in order to capture sub-surface chlorophyll maximums.

4.1 ~~Phytoplankton changes with wave coupling~~

~~Fig. 8 shows the simulated chlorophyll concentration throughout the year for a transect in the off-shelf region running N-S.~~ In both the OCN and WAV simulations the bloom originates in the warmer, southern part of the domain with a strong signal around April followed by a period of elevated concentrations that eventually die out in January. In the northern part of the domain the initial bloom occurs approximately 2 weeks later, with the elevated concentration period ending by November. The bloom is interrupted by storm Hector mid-June and a secondary bloom is clear on the ~~onshelf~~ on-shelf part of the transect ($48\,\mathrm{N}$ to $55\,\mathrm{N}$) at the start of July, which corresponds to the start of the marine heatwave (Fig 3), two weeks after storm Hector. ~~This second peak is also present in observations, though 1 week earlier in the observations (not shown).~~

~~The differences between the two simulations are characterized by a mean delay of in the initial bloom when waves are coupled, as shown in Fig. 10. The~~ The WAV simulations additionally show increased chlorophyll concentration in the secondary late June peak, and then in August and September near the shelf break between $48\,\mathrm{N}$ and $55\,\mathrm{N}$.

By considering the on-shelf, shelf-break and off-shelf regions, as highlighted in Fig. 1, the temporal patterns for the different zones can be assessed. Fig. 9 shows the difference in mean net primary production (NPP) as a time-series. The shallow, sheltered on-shelf region is relatively less affected by the addition of waves into the system, whereas the shelf-break and off-shelf zones have a more pronounced difference. In both these regions there is a negative peak followed by a positive one, highlighting the offset nature of the blooms. In the shelf-break region, after the initial blooms for both models NPP levels are consistently
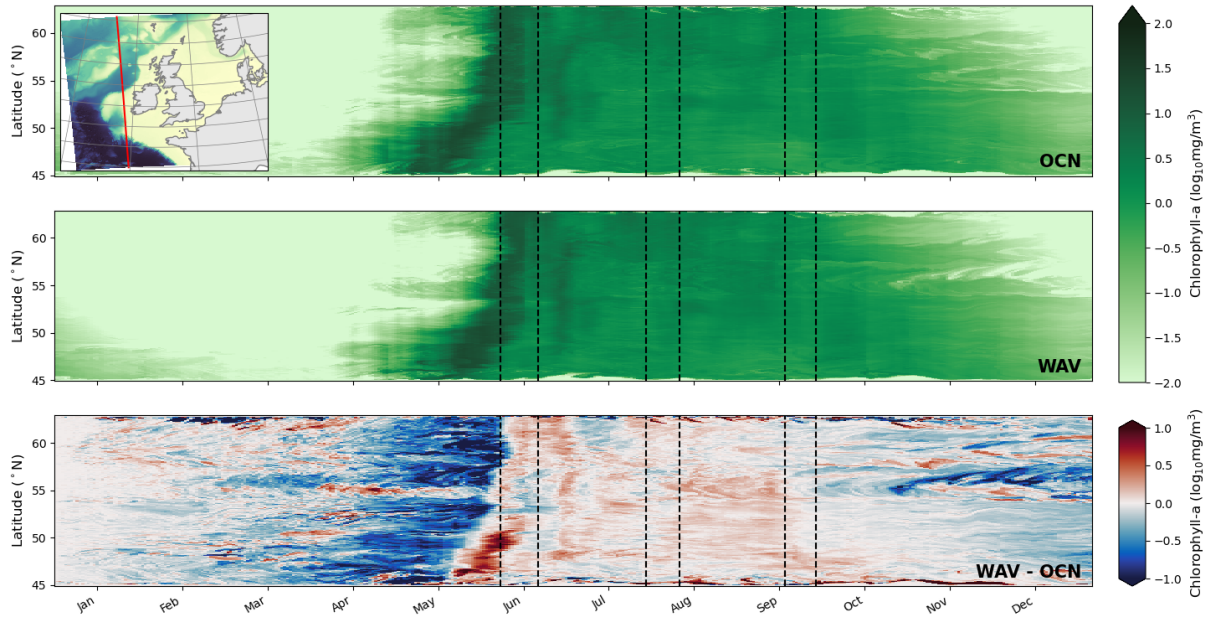
Figure 8. Chlorophyll (averaged over euphotic depth) time/latitude transect along the red line indicated in the top left hand inset for (top) OCN, (middle) WAV, (bottom) WAV-OCN. Black vertical dashed lines show storm periods

higher throughout the summer when waves are included. In off-shelf areas, the offset is greater leading to a larger overall difference in primary production.

4.1 Bloom phenology

Accurately determining the phenology of phytoplankton blooms is challenging, with different methods yielding wildly different results (Brody et al., 2013). Here we used the approach of Jardine et al. (2022) to predict the bloom onset, with the timing defined as the start of exponential growth in the concentration of chlorophyll (used as a proxy for phytoplankton biomass). This is defined to be the time when the change in the concentration of chlorophyll exceeds $0.15\,\mathrm{mg\,m^{-2}\,d^{-1}}$ consistently for 5 consecutive days. This approach performs best with full temporal data coverage, making it ideal to apply to model output but not so useful for patchy satellite data.

By applying this algorithm to both model runs, we see that coupling with waves delays the bloom onset across most of the model domain (Fig. 10). On-shelf, the response to wave coupling is minimal as the shallow waters are already well mixed by
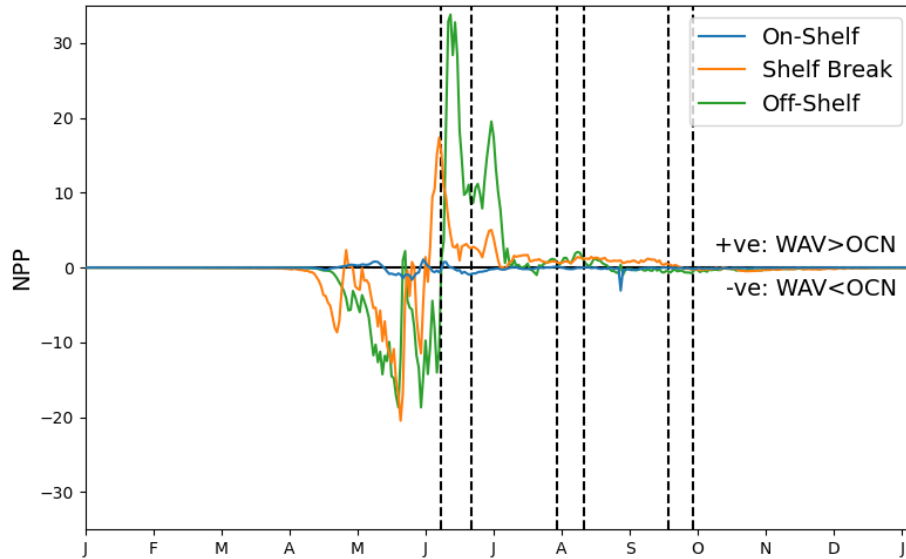
20

Figure 9. Mean difference in NPP between simulations for off-shelf, shelf-break and on-shelf regions as defined in Fig. 1, with storm periods indicated by black vertical dashed lines.

tidal processes, whereas off-shelf bloom onset is typically 1-2 weeks later with larger delays in the south. Across the entire domain there is a mean delay of 3.2 days.

In addition to delaying bloom onset, the yearly total of chlorophyll averaged over the euphotic depth is up to 20 % higher in the high-productivity region along the northern reaches of the shelf break and also in some deeper waters (Fig. 10).

The date of bloom onset in the model runs is later than observations usually suggest. Later model predictions of bloom onset relative to observations have been observed in past NEMO-ERSEM simulations (Skákala et al., 2020) and, in part, stem from the parametrisation of photosynthesis, phytoplankton growth and grazing effects. The biological model is also influenced by biases in the physical model, including temperature, which directly impacts biological rates as well as the timing of stratification; and the ability to accurately represent optically active components, such as coloured dissolved organic matter (cDOM) and suspended particulate matter (SPM), which impact light attenuation. Nevertheless, spatial variability is captured by the model, such as pockets of very late bloom over the shelf; and the later bloom onset along the shelf break north of Scotland and in the open ocean around 51 N. The south-north gradient is also evident in both the model runs and observations, although it is more pronounced in the model.

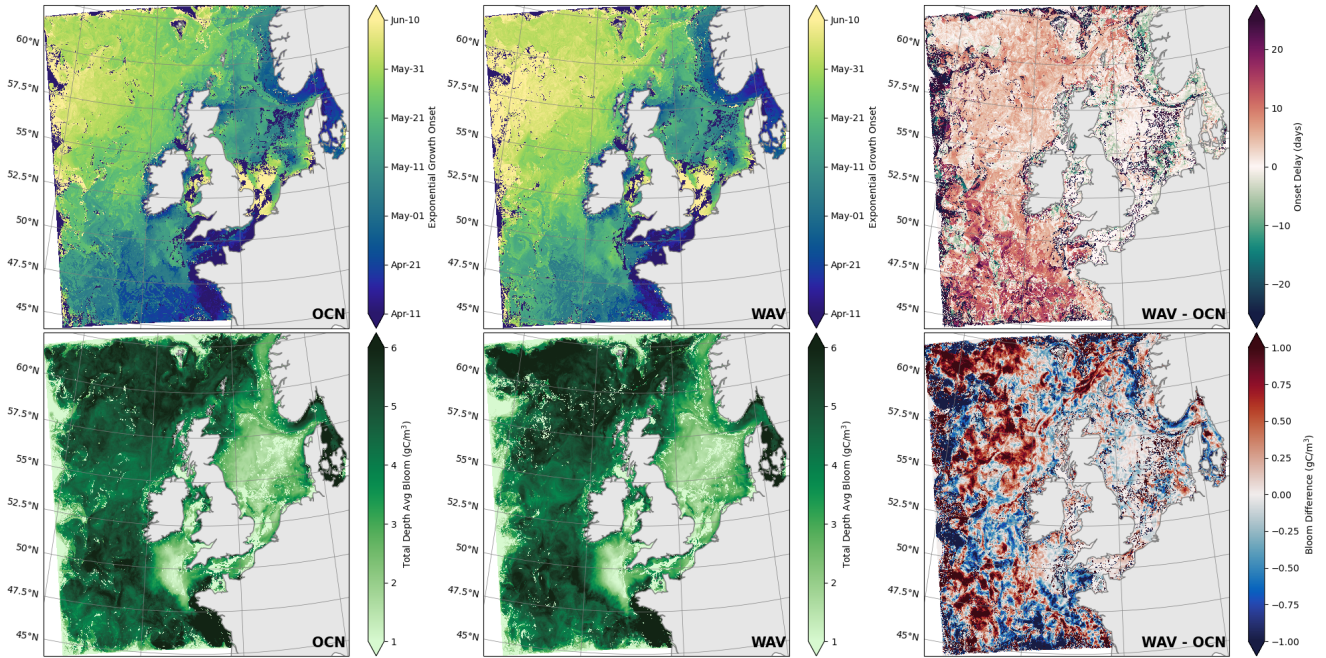**Figure 10.** Date of onset of exponential growth (top) and total NPP over the year averaged to the euphotic depth (bottom) for OCN (left), WAV (middle) and the difference; WAV minus OCN (right).

5 Wave Coupling Mechanisms

In this section, we assess the differences in physics and biogeochemistry between the two model simulations to understand the mechanisms behind the differences seen in Section 4. By running the same physics and biogeochemical model setup with and without wave coupling, we can isolate the effect of wave coupling, independent of the biases in the models relative to
460 observations.

5.1 Physical changes with wave coupling

Figures 11 and 12 show average Hovmöller plots for three distinct regions of the domain; off-shelf, the shelf break and North sea on-shelf region, as defined in Fig. 1. The first (Fig. 11) shows absolute values from the coupled WAV simulation, whilst the second (Fig. 12) shows the difference between the WAV and OCN simulations.

465

The top row in Fig 11 and Fig 12 show ~~similar results to Lewis et al. (2019)~~temperature: when the water column ~~in~~ is stratified, the ocean-wave coupled system is cooler in the mixed layer~~(~~, and warmer below the mixed layer in May-June, before the first summer storm~~)~~, due to increased vertical mixing when treating waves explicitly. Over the shelf region, this signal is also clear at the start of stratification episodes (May and July), but then reverses after strong mixing events~~, unlike~~. This difference

22

470 between the runs when stratified is similar to the results seen in Lewis et al. (2019), ~~where it~~ however in those experiments the stratification remained for the whole season ~~, as the stratification was not disrupted by~~ as there were no disruptions by summer storms in their ~~chosen summer~~ year of study (2017). These mixing events in 2018; (storm Hector (~~13-14~~ 13th-14th June), ~~July 29 storm~~ unnamed storm (29th July), storms Ali and Bronagh ~~18-21 September)~~ (18th-21st September)) are clearly seen through a sudden erosion of stratification in Fig 11. Vertical mixing is increased when coupled with waves (2nd row~~of~~,

475 Fig 12), and the coupled simulations are generally cooler from the surface down to 60 m to 100 m in the off-shelf and shelf-break regions after storms (3rd row, Fig 12). This persists even after stratification has re-formed (end June-July) due to a deeper mixed layer in the coupled runs.

The ~~second row in Fig 11 and Fig 12 shows the main~~ main direct effect of coupling with waves ~~off shelf~~ off-shelf and in the

480 shelf-break is to increase turbulent kinetic energy (TKE) in the ocean, which is related to the change in surface roughness and water-side stress, now calculated by the wave model (Figs 11, 12, 2nd row). On the shelf break, TKE penetrates deeper in the ocean during summer storms, potentially because of the interaction with the bathymetry and breaking of internal waves. This explains the deeper cooling effect of wave coupling in this region.

485 On-shelf in the North Sea, the ~~effect~~ direct effects of wave coupling is more varied, with a decrease in TKE for the main mixing events during the stratification period (Fig 12, rightmost panels). This is likely due to the fact that wave age in the North Sea ~~tend~~ tends to be small as waves there are generated by local wind~~sea~~, not remotely generated swells. Therefore ~~,~~ in this region, and in the case of intense events like the ones responsible for deep mixing, the waves will tend to extract momentum from the atmosphere before it is passed to the ocean, and therefore reduce TKE (Gentile et al., 2021). This explains the warm-

490 ing with wave coupling after mixing events in this region: the mixing in the ocean ~~got less deep~~ has become shallower with wave coupling as waves extract energy from the atmosphere before it is passed to the ocean~~in this region~~.

5.2 Linking physical and biogeochemical changes from wave coupling

Nutrient differences with wave coupling are consistent with temperature changes once ~~the~~ stratification is established (~~Fig 11and~~

495 ~~Fig~~ Figs 11, 12, 3rd row)~~: with decreased off-shelf and shelf break nitrate concentrations as it is consumed by phytoplankton~~. Extra TKE ~~induced~~ introduced by the wave model brings additional nutrients from nitrate-rich deeper layers to the surface, reducing nutrient content in these deeper layers. ~~To the contrary, over the shelf where the impact of TKE is limited even during strong mixing events, nitrates are only slightly reduced in the WAV simulation, though the levels are very low anyway. Each storm imprint~~ Each storm is also clearly seen in ~~all~~ the off-shelf and shelf-break profiles, increasing nutrient concentration

500 near the surface, and this effect is stronger with wave coupling. ~~On the shelf break, where TKE mixing affects deeper layers, phytoplankton is distributed more evenly throughout the column and the euphotic zone is deeper than . The additional mixing in this region results in more nutrients throughout depth, and increased chlorophyll throughout the column (Fig 11 and Fig 12,~~
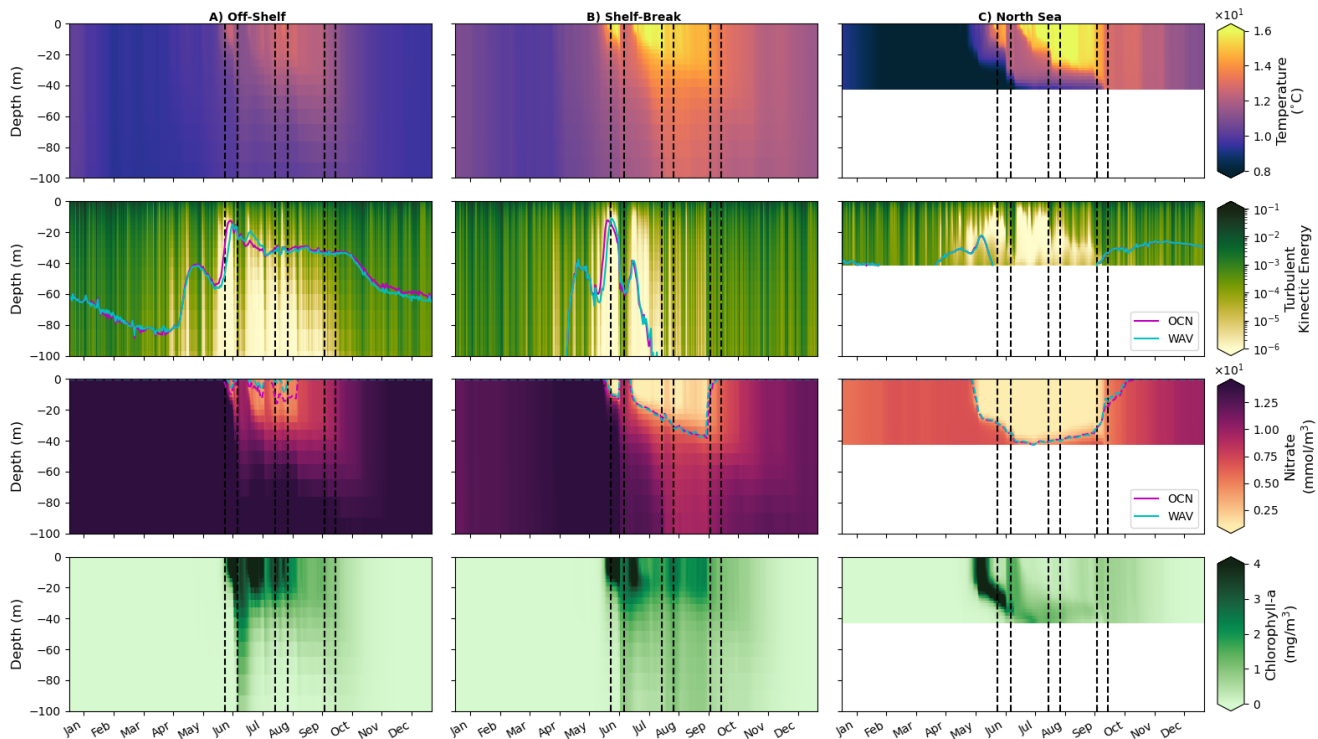
Figure 11. Hovmöller plots (depth/time) of WAV output for potential temperature, turbulent kinetic energy, nitrate, chlorophyll and light availability for (left) off-shelf, (middle) shelf-break and (right) ~~on-shelf~~ North Sea regions defined in Fig. 1. Dashed lines indicate ~~Magenta~~ storm periods. The magenta (OCN) ~~/Cyan~~ and cyan (WAV) time series show euphotic depth (1 % of surface light) in the second row and nutricline depth (3 μmol kg^{-1} threshold) in the third.

~~4th row). Off shelf, chlorophyll is only increased at depth under the euphotic zone due to increased mixing. Off-shelf, increased nutrient concentration near the surface may be compensated by decreased light availability with a deeper mixed layer.~~

505　　At the onset of stratification (~~April-May south off-shelf and~~ May-June~~in the North~~), the pattern in nitrate near the surface is ~~anticorrelated~~ anti-correlated with the pattern of ~~chlorlophyll-a content of~~ chlorophyll-a content (Fig 11 ~~this~~). This pattern is controlled by the consumption of nitrate by the spring phytoplankton bloom, which occurs later with wave coupling ~~. After this, cholophyll-a~~ (Fig 11, 4th row). From late June, chlorophyll-a content under the mixed layer is generally larger when coupled to the wave model, illustrative of a stronger export of phytoplankton ~~at~~ to depth with stronger TKE. The additional mixing in

510　　these regions results in increased chlorophyll throughout the column (Figs 11, 12, 4th row). Increased nutrient concentrations near the surface after mixing events may be offset by reduced light availability due to a deeper mixed layer and enhanced vertical mixing that transports chlorophyll out of the euphotic zone.
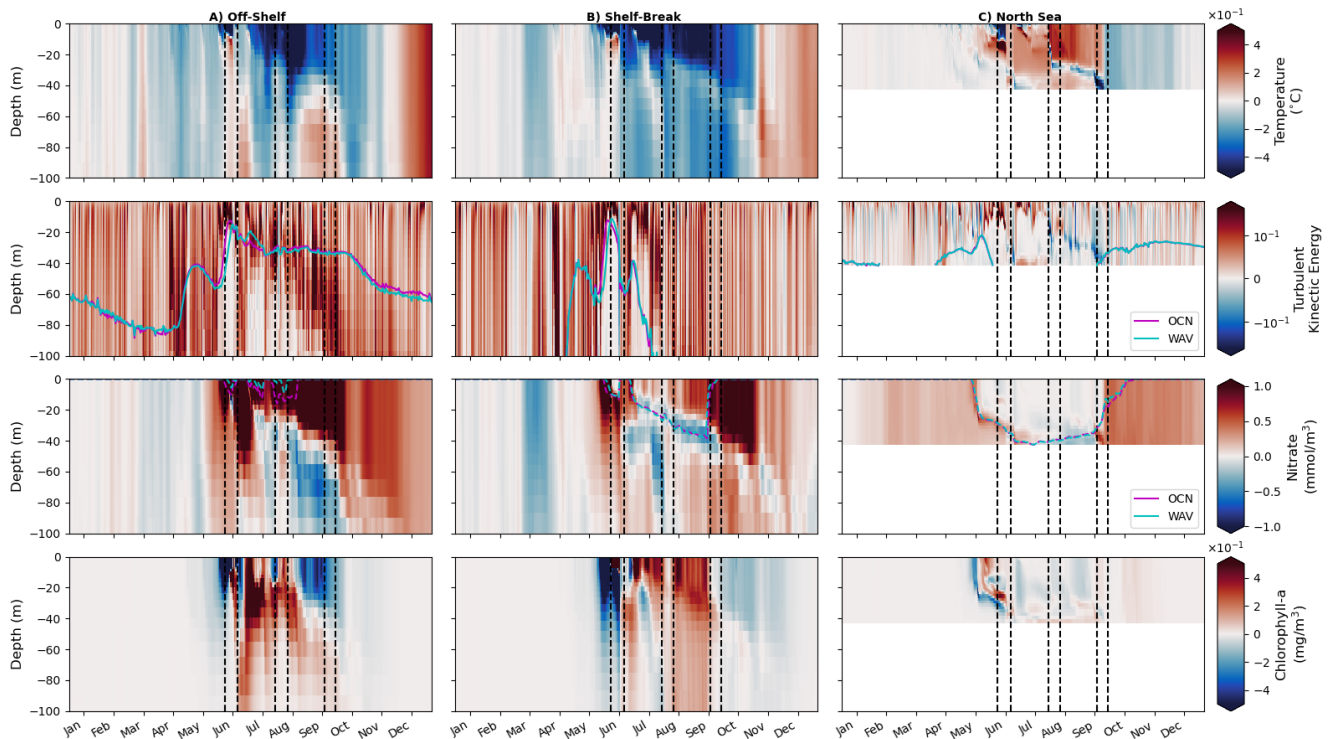
Figure 12. Hovmöller plots (depth/time) of WAV-OCN for potential temperature, turbulent kinetic energy, nitrate, chlorophyll and light availability for (left) off-shelf, (middle) shelf-break and (right) on-shelf North Sea regions defined in Fig. 1. Magenta (OCN)/Cyan (WAV) time series show euphotic depth (1 % of surface light) in the second row and nutricline ($3\,\mu\mathrm{mol\,kg}^{-1}$ threshold) in the third.

The delay in phytoplankton bloom with wave coupling can be explained by a combination of the change in light availability
515   and temperature for the phytoplankton at the ~~infancy stage~~ early stages of the bloom, both of which impact growth rate and are reduced by wave mixing at the time of bloom onset. At the ~~onset of the~~ beginning of the summer stratification period, the formation of ~~the~~ a shallower mixed layer helps ~~maintain~~ retain phytoplankton in the euphotic zone~~. Phytoplankton can then~~, allowing phytoplankton to bloom because of high nutrient concentration and light availability. Then, ~~phytoplankton becomes~~ throughout the growing season phytoplankton become limited by nutrient availability and the bloom reduces. Coupling to the
520   wave model consistently reduces stratification in April-May (Fig. 13) by increasing TKE, which decreases temperature and leads to phytoplankton going through deeper cycles in the emergent mixed layer with longer time in ~~deeper~~ regions where light availability is lower. This delays the phytoplankton bloom, which happens 1-2 weeks later with wave model coupling.

~~In the North Sea, phytoplankton delay is still visible but the effect is less strong , as light is actually available throughout~~
525   ~~the column outside the phytoplankton bloom~~ On the other hand, the impact of TKE is limited on the shelf even during strong mixing events. By the time storm Hector crosses the domain, phytoplankton have already consumed most of the existing stock
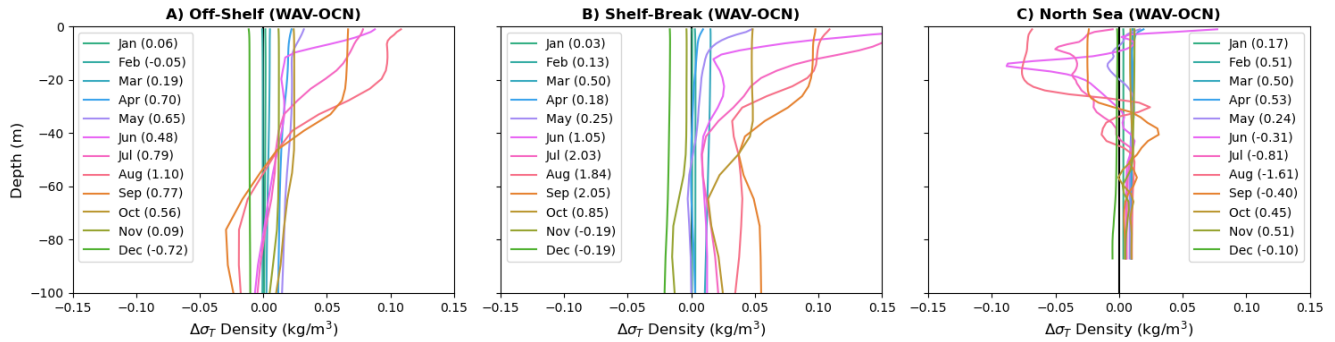
Figure 13. Difference in density (~~kg/m3~~ kg/m^3) stratification profiles in the upper ~~150m~~ 150m throughout the year for the three regions. Density given in $\sigma_T(=\sigma-1000)$ coordinates, with the total difference throughout the column for each month shown in parenthesis.

of nitrate and there is no nutrient-rich deep layer to resupply. Interestingly, each phytoplankton 'bloom' associated with the strong mixing events and termination of marine heatwaves is reduced by wave coupling~~, since the wave effect on these events is to reduce mixing by extracting atmospheric momentum by~~. In the coupled case, momentum from the atmosphere is used to grow young waves. This delays the transfer of energy from atmosphere to ocean. In the ocean-only simulation, where waves are not explicitly included, the energy can abruptly mix the water column without this intermediate step. The apparent summer/autumn blooms after these events are not necessarily new growth, with increased surface chlorophyll the result of the mixing of the sub-surface chlorophyll maximum up from the nutricline to the surface, giving the appearance of a bloom.

5.3 Storm impact

6 ~~Linking wave and phytoplankton activities~~

~~The relationship between wave activity and phytoplankton found in Fig 2 can be better understood from our analysis. Fig 4 showed that a mid-June storm tended to decrease phytoplankton activity off-shelf and increase it on the shelf break. The model was in agreement with this, but its response is stronger because this storm happens when chlorophyll levels are elevated in northern off-shelf regions in the model. Fig 11 shows the storm effect in the model is to~~ There is a clear difference in response to storms between the deeper, open ocean and the sheltered shallow on-shelf area of the North Sea. Off-shelf, the phytoplankton sit near the surface so when the storms pass over the region they mix the chlorophyll from 0 m to 20 m down to about 100 m, ~~hence the strong decrease in phytoplankton near the surface.~~

~~However, southwest of Ireland, both the observation and model have little activity before the storm, and increased activity after the storm. In this region, phytoplankton is limited by nutrients , which~~ as seen in Fig 11, row 4. At the same time nutrients are brought nearer the surface by storm mixing because injected TKE reaches nutrient-rich water below the nutricline ~~, as shown in~~ (Fig. 11 ~~(shelf-break region).~~

26

~~In the North Sea, the model shows a stronger chlorophyll levels than the observations. However, for the July~~ , row 3). The stage of the phytoplankton bloom at which the storm occurs also affects the response. At the time of the second storm, the ~~model agrees with the observations and doesn't increase in concentration. In this region, model~~ phytoplankton levels have decreased from the initial bloom, as such the mixing has a similar effect to the first storm, but of a smaller magnitude.

In contrast, on-shelf the profiles of chlorophyll and nutrients ~~(Fig. 11)~~ indicate that the bloom starts near the surface and then moves deeper in the watercolumn, where nutrients are still available ~~. In the model, the storm happens when~~ (Fig. 11). When the first storm occurs the chlorophyll maximum is still at depth, ~~bringing it back to the surface. In July, however,~~ so the mixing spreads the bloom back up through the water column. By the time of the second summer storm in July, nutrients are depleted throughout the column and ~~there is very little chlorophyll in the column~~ the phytoplankton bloom has finished, so the storm has ~~no impact. Therefore, the difference in the North Sea between model and observations in the June storm (Hector)is most likely due to the bloom being too late in the model.~~ a limited impact.

~~In July, the off-shelf response of the model~~

As previously shown in the satellite measurements, the passage of storms across the domain has a large impact on the distribution of chlorophyll (Fig 4). The results from the models for the same period are shown in Fig 14. Due to the biases highlighted in section 4.1, the chlorophyll concentrations are generally higher in the models relative to the satellite observations, meaning Storm Hector has a larger impact on sea surface chlorophyll concentrations in the models than it does in the observations. Nevertheless, the spatial pattern of the response to the storm is ~~too strong and suggests that the nutricline may be too shallow~~ similar between the models and the observations, with a suppression of phytoplankton activity off-shelf ~~in the model.~~

~~Finally,~~ and increased activity on-shelf. For the July storm, the models capture the increase in the concentration of chlorophyll on the western and northern edges of the North Sea (Fig 14), whilst there is little effect observed in the satellite measurements. For storms Ali and Bronagh, the north-south gradient in the response in the ~~model, the first autumn storm (Ali/Bronagh) sees a small increase in chlorophyll in the~~ North ~~sea by increasing nutrient availability near the surface, but TKE does not quite reach the whole depth, and~~ Sea is well captured by the ~~chlorophyll concentration is underestimated. There are several feedbacks between the wave~~ model, though it is not as intense as the earlier storms.

One element captured by satellite observations but not by either of the models is an autumn bloom in the southern North Sea, that appears to be elevated by the passing of the autumn storms Ali and Bronagh (Fig 4, row 3). Whilst it is possible that the satellite measurements are not representative, the absence of a bloom in the models is more likely to be due to the biogeochemical model not encountering the right physical conditions. The issue could be related to the temperature bias, or due to feedback mechanisms between the waves and atmosphere that are not represented by the models~~that could affect this~~, such as the change in surface roughness due to young waves.
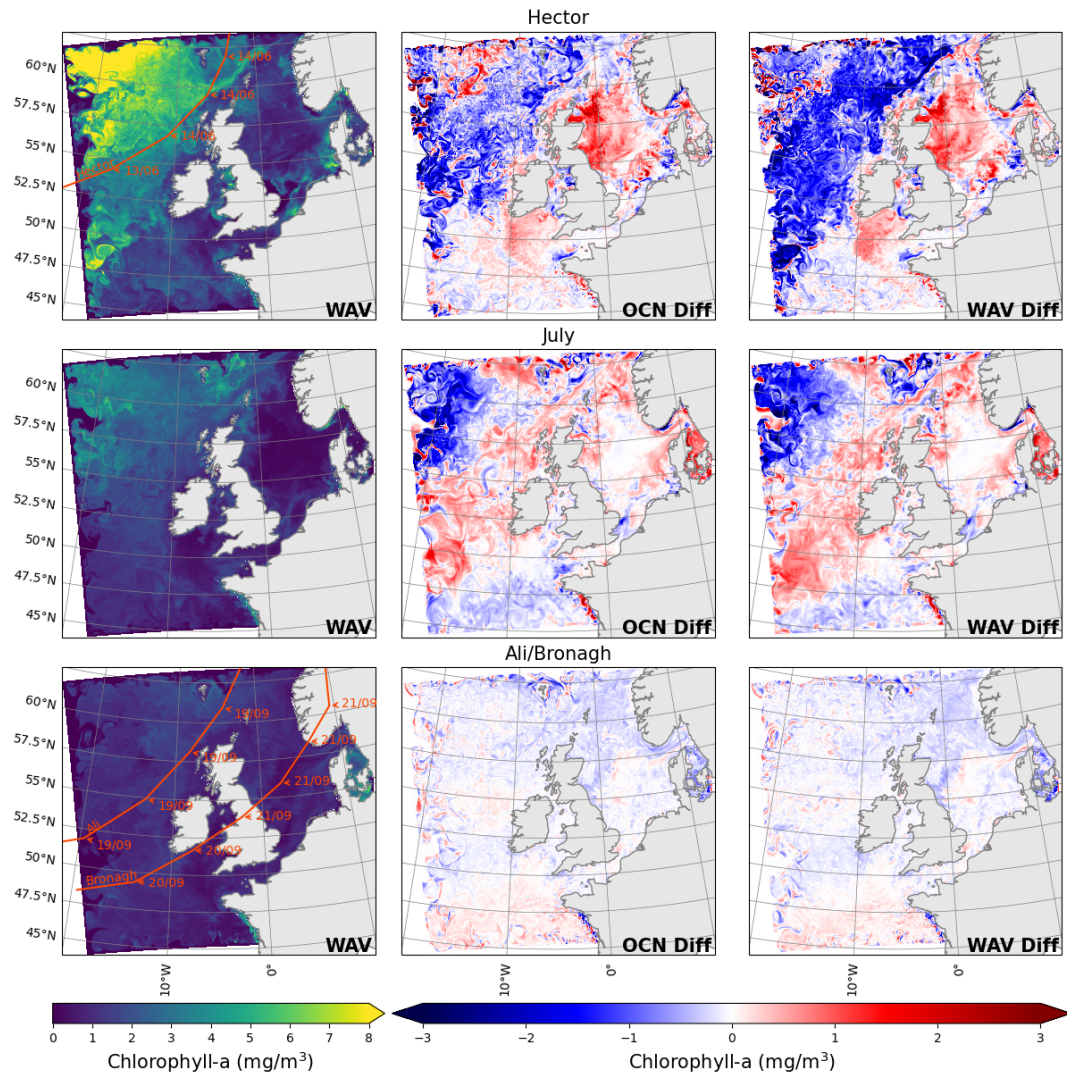
Figure 14. Mean chlorophyll in the five days before the storm from the ocean-biogeochemistry model (left), the difference between the mean of the five days after the storm and the mean of the five days before the storm from the ocean-biogeochemistry model (middle) and the ocean-wave-biogeochemistry model (right), for storm Hector (top), July storm (middle) and storms Ali and Bronagh (bottom). The start of the five days before and the end of the five days after the storms are highlighted in Figure 3 as vertical bars.
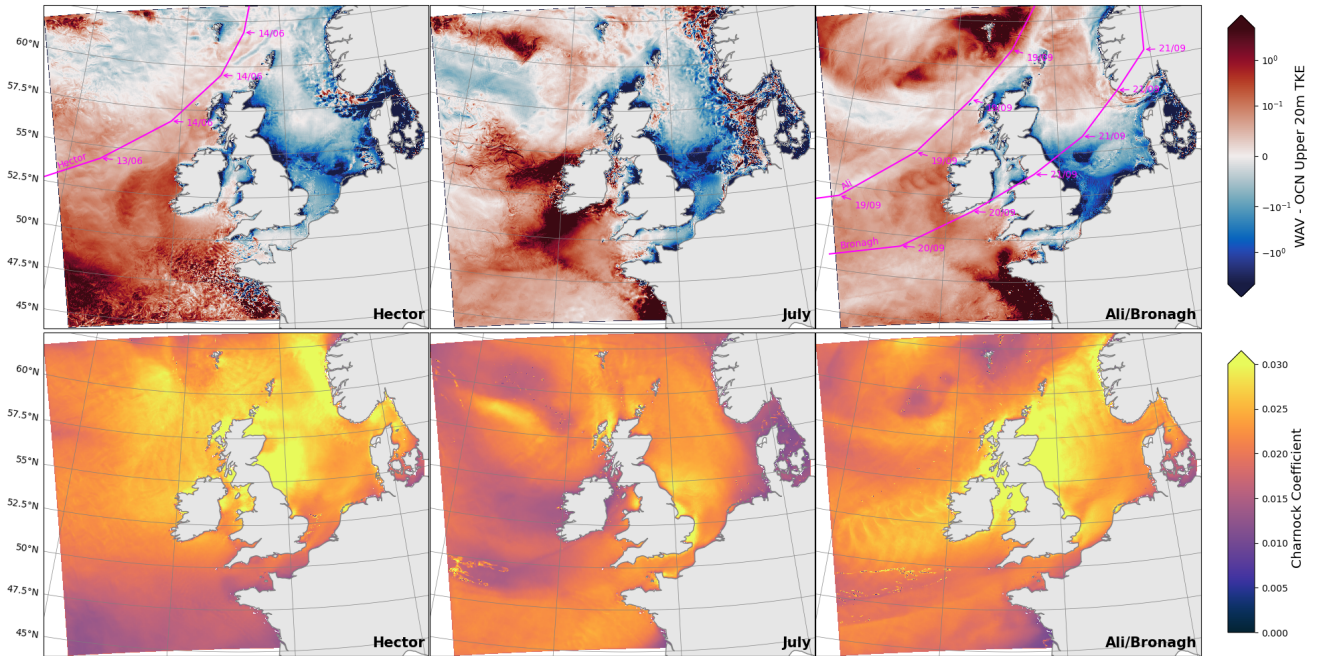
28

Figure 15. Difference in upper 20 m turbulent kinetic energy (TKE) between simulations (top) and the Charnock coefficient from wave model (bottom) on; 14/6 for storm Hector (left), 29/7 for the July storm (middle) and 20/9 for storms Ali/Bronagh (right). Storm paths are shown in magenta where available.

The difference in TKE between the model simulations as a result of the storms is shown in Fig. 15. The dominant impact of wave coupling is an increase in mixing energy across the western half of the domain where the storms originate, whereas east of the British Isles in the sheltered areas of the North sea, especially the south, there is a reduction in TKE due to the wave coupling.

Also shown in Fig. 15 is the Charnock coefficient, a parameter that relates the sea surface roughness to wind friction velocity. A high Charnock value is associated with young waves and high wind speed (Moon et al., 2004). In the WAV simulation the Charnock coefficient and TKE are correlated, with temporal Pearson correlation values in excess of 0.6 across the domain.

In the wave coupled system, the high Charnock value in the North sea during storms is due to a large proportion of the wind stress energy being used to create growing waves, whereas in the parametrised OCN simulation the wind stress energy is instead transferred directly into the ocean. The difference in energy transfer results in the differences in TKE seen in Fig. 15, but the impact on phytoplankton in the North sea is minimal as the region is shallow and already well mixed by tidal processes.

29

6 Conclusion

This paper is the first ~~usage~~ use of a km scale coupled wave-hydrodynamic-ecosystem model. ~~We demonstrate the~~ Whilst simulations suffered from a systematic warm bias, the results supports similar findings to the studies of Liu et al. (2025); Tensubam et al. (20... . The use of a twin study isolated the mechanistic impact of waves on shelf-seas ecosystems, ~~and investigate~~ allowing an investigation into how seasonal productivity can be altered by the sea state.

~~Our~~ The study identified regional and seasonal variations in the response of phytoplankton to wave activity: during the bloom (in March-April in the observations, April-June in the model), with enhanced wave activity ~~off shelf~~ off-shelf or near the shelf break ~~induces a mix down~~ inducing mixing of the surface bloom down into deeper waters, and the chlorophyll concentration near the surface is reduced.

On-shelf, enhanced wave activity tends to generally increase chlorophyll activity near the surface from July to September, likely because light is available throughout the water column, and wave mixing helps mix nutrients from rich to poor regions~~(either~~ . This could either occur through advection of nutrient-rich river plumes or ~~vertically~~ through vertical mixing if the injection of TKE is deep enough and nutrients are still available near the bottom of the sea, which is possibly not the case in May-June (Fig 2).

~~Finally, phytoplankton activity also increases off shelf in the southwest part of the domain in June-September. The model's response to storms in July and September suggests this is through bringing nutrients up from below the nutricline, when phytoplankton activity is very low.~~

This paper also investigated the effects of explicitly treating wave input to the ocean as a separate model coupled to the ocean with a ~~1.5km~~ 1.5 km grid spacing. The main findings depend on the region of interest:

– ~~off-shelf~~ Off-shelf on the Atlantic side of the domain, explicit coupling with waves increases the injection of turbulent kinetic energy into the ocean across depth (Fig 12). This reduces stratification at the start of the growing season, meaning that phytoplankton is not trapped as close to the surface~~by an emergent stratification~~, and gets less light through deeper mixing cycles induced by stronger TKE. The bloom is therefore triggered later with the wave model (Fig 10). Total chlorophyll concentration and NPP are increased in summer, ~~where~~ as stronger TKE injection leads to more intense phytoplankton secondary blooms

– ~~on~~ On the shelf-break, the conclusions are similar, ~~but~~ with the increase in summer production is more pronounced than off-shelf.

– ~~on shelf~~ On-shelf, the changes are smaller for ~~various reasons: outside bloom season,~~ several reasons; Firstly outside the bloom season the euphotic depth is close to the actual shelf depth in the North Sea, so additional mixing does not affect the phytoplankton bloom as much. Second, the North Sea is sheltered by the British Isles and has younger waves than the Atlantic side. Young waves extract momentum from the atmosphere before ~~it is passed~~ passing it to the ocean, and

30

630 ~~reduce the amount~~ delay the transfer of TKE in the ocean~~, this is clearly ~~. This is visible during summer storms (Fig 15), when marine heatwave stratification breaks~~: the mixing is less strong with the wave model and the various events of elevated chlorophyll concentration following these mixing events are less intense~~. In the WAV case, the waves delay transfer of momentum and spread the event over a longer time acting to 'flatten the curve'. Thus the mixing event is less sharp and intense, and the elevated chlorophyll concentrations less peaked.

635 ~~In line with previous findings, this study shows that coupling with a wave model improves the quality of the hydrodynamical model (Berthou et al., 2025b). However, it deteriorates phytoplankton activity: ERSEM has always been developed in a standalone ocean framework and may require further developments when used in a coupled system.~~

Future work will include ~~comparing these simulations with~~ fixing the temperature bias from the surface forcing and evaluating a fully coupled simulation which includes a regional configuration of the Met Office atmosphere and land system: the ~~physics~~
640 ~~only configuration~~ physics-only configuration for which is documented in a companion paper (Berthou et al., 2025a). In the present work, the ecosystem model does not feedback ~~on~~ to the physical system: future work will include chlorophyll feedback on light penetration in the physical ocean building on Skákala et al. (2020), and ~~sending surface chlorophyll back~~ providing surface chlorophyll values to the atmosphere for the calculation of surface albedo. Rivers will also ~~get~~ be coupled to the ocean, ~~and variable nutrient concentration eventually added too~~with the target of enabling variable nutrient loads to enter the ocean
645 through the river instead of the current climatological input.

A fully coupled system will enable the study of compound events across land and marine environments in a changing climate. Representing the ocean colour feedback on the ocean and atmosphere was indeed recently shown to be important for climate projections in the Mediterranean, with resulting SST changes up to ~~1°C~~1 °C (Zhang et al., 2025).

650 **Code and Data Availability**

All scripts used to generate the biogeochemical input data are provided here: https://github.com/dalepartridge/AMM15_BGC_setup. The satellite data is available through OC-CCI (Sathyendranath et al., 2019)(Sathyendranath et al., 2023). The Met Office wave regional reanalysis is available from Copernicus: https://doi.org/10.48670/moi-00060. Given the size of 1-year of model output of this model, the data is stored locally and is available upon request by the authors.

655 **Author Contribution**

RM conducted analysis of observations vs wave data. DP set up and ran the model simulations with support from JMC and SB. Model analysis was conducted by DP and SB. Comparison between the model and EN4 profiles was done by JR. JC performed a literature review and biogeochemistry expertise. LB provided significant insight and expertise on wave processes. HL proposed and initiated the project. DP led the writing of the manuscript, with contributions to the writing and editing from
660 all authors.

Competing Interests

The authors declare that they have no conflict of interest.

Acknowledgments

References

Alari, V., Staneva, J., Øyvind Breivik, Bidlot, J.-R., Mogensen, K., and Janssen, P.: Surface wave effects on water temperature in the Baltic Sea: simulations with the coupled NEMO-WAM model, Ocean Dynamics, 66, 917–930, https://doi.org/10.1007/s10236-016-0963-x, 2016.

Babin, S. M., Carton, J. A., Dickey, T. D., and Wiggert, J. D.: Satellite evidence of hurricane-induced phytoplankton blooms in an oceanic desert, Journal of Geophysical Research: Oceans, 109, https://doi.org/https://doi.org/10.1029/2003JC001938, 2004.

Behrenfeld, M. J.: Abandoning Sverdrup's Critical Depth Hypothesis on phytoplankton blooms, Ecology, 91, 977–989, https://doi.org/https://doi.org/10.1890/09-1207.1, 2010.

Berthou, S., Mahmood, S., Makrygianni, N., Castillo, J. M., Sanchez, C., Arnold, A., Lewis, H., Fraser-Leonhardt, V., and Tinker, J.: Km-scale regional coupled system in the Northwest European shelf for weather and climate applications: RCS-UKC4, QJRMS, p. 20, 2025a.

Berthou, S., Siddorn, J., Fraser-Leonhardt, V., Traon, P.-Y. L., and Hoteit, I.: Towards Earth system modelling: coupled ocean forecasting, State of the Planet, 5-opsr, 20, https://doi.org/10.5194/sp-5-opsr-20-2025, 2025b.

Brody, S. R., Lozier, M. S., and Dunne, J. P.: A Comparison of Methods to Determine Phytoplankton Bloom Initiation, Journal of Geophysical Research: Oceans, 118, 2345–2357, https://doi.org/10.1002/jgrc.20167, 2013.

Bruciaferri, D., Tonani, M., Lewis, H. W., Siddorn, J. R., Saulter, A., Castillo Sanchez, J. M., Valiente, N. G., Conley, D., Sykes, P., Ascione, I., and McConnell, N.: The Impact of Ocean-Wave Coupling on the Upper Ocean Circulation During Storm Events, Journal of Geophysical Research: Oceans, 126, e2021JC017 343, https://doi.org/https://doi.org/10.1029/2021JC017343, 2021.

Bruggeman, J. and Bolding, K.: A general framework for aquatic biogeochemical models, Environmental Modelling & Software, 61, 249–265, https://doi.org/https://doi.org/10.1016/j.envsoft.2014.04.002, 2014.

Butenschön, M., Clark, J., Aldridge, J. N., Allen, J. I., Artioli, Y., Blackford, J., Bruggeman, J., Cazenave, P., Ciavatta, S., Kay, S., Lessin, G., van Leeuwen, S., van der Molen, J., de Mora, L., Polimene, L., Sailley, S., Stephens, N., and Torres, R.: ERSEM 15.06: a generic model for marine biogeochemistry and the ecosystem dynamics of the lower trophic levels, Geoscientific Model Development, 9, 1293–1339, https://doi.org/10.5194/gmd-9-1293-2016, 2016.

Cavaleri, L., Fox-Kemper, B., and Hemer, M.: Wind Waves in the Coupled Climate System, Bulletin of the American Meteorological Society, 93, 1651 – 1661, https://doi.org/10.1175/BAMS-D-11-00170.1, 2012.

Couvelard, X., Lemarié, F., Samson, G., Redelsperger, J.-L., Ardhuin, F., Benshila, R., and Madec, G.: Development of a two-way-coupled ocean–wave model: assessment on a global NEMO(v3.6)–WW3(v6.02) coupled configuration, Geoscientific Model Development, 13, 3067–3090, https://doi.org/10.5194/gmd-13-3067-2020, 2020.

Craig, P. D. and Banner, M. L.: Modeling Wave-Enhanced Turbulence in the Ocean Surface Layer, Journal of Physical Oceanography, 24, 2546 – 2559, https://doi.org/10.1175/1520-0485(1994)024<2546:MWETIT>2.0.CO;2, 1994.

Cushing, D.: Plankton Production and Year-class Strength in Fish Populations: an Update of the Match/Mismatch Hypothesis, vol. 26 of *Advances in Marine Biology*, pp. 249–293, Academic Press, https://doi.org/https://doi.org/10.1016/S0065-2881(08)60202-3, 1990.

Cyr, F., Lewis, K., Bélanger, D., Regular, P., Clay, S., and Devred, E.: Physical controls and ecological implications of the timing of the spring phytoplankton bloom on the Newfoundland and Labrador shelf, Limnology and Oceanography Letters, 9, 191–198, https://doi.org/https://doi.org/10.1002/lol2.10347, 2024.

Filipot, J.-F., Ardhuin, F., and Babanin, A. V.: A unified deep-to-shallow water wave-breaking probability parameterization, Journal of Geophysical Research: Oceans, 115, 2010.

Gentile, E. S., Gray, S. L., Barlow, J. F., Lewis, H. W., and Edwards, J. M.: The Impact of Atmosphere–Ocean–Wave Coupling on the Near-Surface Wind Speed in Forecasts of Extratropical Cyclones, Boundary-Layer Meteorology, 180, 105–129, https://doi.org/10.1007/s10546-021-00614-4, 2021.

Good, S. A., Martin, M. J., and Rayner, N. A.: EN4: Quality controlled ocean temperature and salinity profiles and monthly objective analyses with uncertainty estimates, Journal of Geophysical Research: Oceans, 118, 6704–6716, https://doi.org/https://doi.org/10.1002/2013JC009067, 2013.

Graham, J. A., O'Dea, E., Holt, J., Polton, J., Hewitt, H. T., Furner, R., Guihou, K., Brereton, A., Arnold, A., Wakelin, S., Castillo Sanchez, J. M., and Mayorga Adame, C. G.: AMM15: a new high-resolution NEMO configuration for operational simulation of the European north-west shelf, Geoscientific Model Development, 11, 681–696, https://doi.org/10.5194/gmd-11-681-2018, 2018a.

Graham, J. A., Rosser, J. P., O'Dea, E., and Hewitt, H. T.: Resolving Shelf Break Exchange Around the European Northwest Shelf, Geophysical Research Letters, 45, 12,386–12,395, https://doi.org/https://doi.org/10.1029/2018GL079399, 2018b.

Hasselmann, K.: Wave-driven inertial oscillations, Geophysical Fluid Dynamics, 1, 463–502, https://doi.org/10.1080/03091927009365783, 1970.

Hasselmann, S., Hasselmann, K., Allender, J., and Barnett, T.: Computations and parameterizations of the nonlinear energy transfer in a gravity-wave specturm. Part II: Parameterizations of the nonlinear energy transfer for application in wave models, Journal of Physical Oceanography, 15, 1378–1391, 1985.

Hobday, A. J., Oliver, E. C., Gupta, A. S., Benthuysen, J. A., Burrows, M. T., Donat, M. G., Holbrook, N. J., Moore, P. J., Thomsen, M. S., Wernberg, T., and Smale, D. A.: Categorizing and naming marine heatwaves, Oceanography, 31, 162–173, https://doi.org/10.5670/oceanog.2018.205, 2018.

Huisman, J., van Oostveen, P., and Weissing, F. J.: Critical depth and critical turbulence: Two different mechanisms for the development of phytoplankton blooms, Limnology and Oceanography, 44, 1781–1787, https://doi.org/https://doi.org/10.4319/lo.1999.44.7.1781, 1999.

Jardine, J. E., Palmer, M., Mahaffey, C., Holt, J., Wakelin, S., and Artioli, Y.: Climatic Controls on the Spring Phytoplankton Growing Season in a Temperate Shelf Sea, Journal of Geophysical Research: Oceans, 127, e2021JC017 209, https://doi.org/https://doi.org/10.1029/2021JC017209, 2022.

Ji, R., Edwards, M., Mackas, D. L., Runge, J. A., and Thomas, A. C.: Marine plankton phenology and life history in a changing climate: current research and future directions, Journal of Plankton Research, 32, 1355–1368, https://doi.org/10.1093/plankt/fbq062, 2010.

Jr., W. J. P. and Moskowitz, L.: A proposed spectral form for fully developed wind seas based on the similarity theory of S. A. Kitaigorodskii, Journal of Geophysical Research (1896-1977), 69, 5181–5190, https://doi.org/https://doi.org/10.1029/JZ069i024p05181, 1964.

Komen, G. J., Cavaleri, L., Donelan, M., Hasselmann, K., Hasselmann, S., and Janssen, P. A. E. M.: Dynamics and modelling of ocean waves, Cambridge University Press, 1994.

Lenhart, H.-J., Mills, D. K., Baretta-Bekker, H., van Leeuwen, S. M., van der Molen, J., Baretta, J. W., Blaas, M., Desmit, X., Kühn, W., Lacroix, G., Los, H. J., Ménesguen, A., Neves, R., Proctor, R., Ruardij, P., Skogen, M. D., Vanhoutte-Brunier, A., Villars, M. T., and Wakelin, S. L.: Predicting the consequences of nutrient reduction on the eutrophication status of the North Sea, Journal of Marine Systems, 81, 148–170, https://doi.org/https://doi.org/10.1016/j.jmarsys.2009.12.014, contributions from Advances in Marine Ecosystem Modelling Research II 23-26 June 2008, Plymouth, UK, 2010.

Lewis, H. W., Castillo Sanchez, J. M., Siddorn, J., King, R. R., Tonani, M., Saulter, A., Sykes, P., Pequignet, A.-C., Weedon, G. P., Palmer, T., Staneva, J., and Bricheno, L.: Can wave coupling improve operational regional ocean forecasts for the north-west European Shelf?, Ocean Science, 15, 669–690, https://doi.org/10.5194/os-15-669-2019, 2019.

Li, J.-G.: Propagation of ocean surface waves on a spherical multiple-cell grid, Journal of Computational Physics, 231, 8262–8277, https://doi.org/https://doi.org/10.1016/j.jcp.2012.08.007, 2012.

Liu, X., Pu, X., Qu, D., and Xu, Z.: The role of wave-induced mixing in spring phytoplankton bloom in the South Yellow Sea, Marine Pollution Bulletin, 211, 117 374, https://doi.org/https://doi.org/10.1016/j.marpolbul.2024.117374, 2025.

Madec, G., Delecluse, P., Imbard, M., and Levy, C.: OPA 8 Ocean General Circulation Model - Reference Manual, Tech. rep., LODYC/IPSL Note 11, 1998.

McEvoy, A. J., Atkinson, A., Airs, R. L., Brittain, R., Brown, I., Fileman, E. S., Findlay, H. S., McNeill, C. L., Ostle, C., Smyth, T. J., et al.: The Western Channel Observatory: a century of physical, chemical and biological data compiled from pelagic and benthic habitats in the western English Channel, Earth System Science Data, 15, 5701–5737, 2023.

Moon, I.-J., Ginis, I., and Hara, T.: Effect of Surface Waves on Charnock Coefficient under Tropical Cyclones, Geophysical Research Letters, 31, https://doi.org/10.1029/2004GL020988, 2004.

O'Dea, E. J., Arnold, A. K., Edwards, K. P., Furner, R., Hyder, P., Martin, M. J., Siddorn, J. R., Storkey, D., While, J., Holt, J. T., and Liu, H.: An operational ocean forecast system incorporating NEMO and SST data assimilation for the tidally driven European North-West shelf, Journal of Operational Oceanography, 5, 3–17, https://doi.org/10.1080/1755876X.2012.11020128, 2012.

Phillips, O. M.: The dynamics of the upper ocean, (2nd ed. Cambridge), p. 336, 1977.

Polton, J., Harle, J., Holt, J., Katavouta, A., Partridge, D., Jardine, J., Wakelin, S., Rulent, J., Wise, A., Hutchinson, K., Byrne, D., Bruciaferri, D., O'Dea, E., Dominicis, M. D., Mathiot, P., Coward, A., Yool, A., Palmiéri, J., Lessin, G., Mayorga-Adame, C. G., Guennec, V. L., Arnold, A., and Rousset, C.: Reproducible and relocatable regional ocean modelling: fundamentals and practices, Geoscientific Model Development, 2023.

Powley, H. R., Bruggeman, J., Hopkins, J., Smyth, T., and Blackford, J.: Sensitivity of Shelf Sea Marine Ecosystems to Temporal Resolution of Meteorological Forcing, Journal of Geophysical Research: Oceans, 125, e2019JC015 922, https://doi.org/10.1029/2019JC015922, 2020.

Powley, H. R., Polimene, L., Torres, R., Al Azhar, M., Bell, V., Cooper, D., Holt, J., Wakelin, S., and Artioli, Y.: Modelling terrigenous DOC across the north west European Shelf: Fate of riverine input and impact on air-sea CO2 fluxes, Science of the Total Environment, 912, 168 938, 2024.

Racault, M.-F., Le Quéré, C., Buitenhuis, E., Sathyendranath, S., and Platt, T.: Phytoplankton phenology in the global ocean, Ecological Indicators, 14, 152–163, 2012.

Rascle, N., Ardhuin, F., Queffeulou, P., and Croizé-Fillon, D.: A global wave parameter database for geophysical applications. Part 1: Wave-current–turbulence interaction parameters for the open ocean based on traditional parameterizations, Ocean Modelling, 25, 154–171, 2008.

Reffray, G., Bourdalle-Badie, R., and Calone, C.: Modelling turbulent vertical mixing sensitivity using a 1-D version of NEMO, Geoscientific Model Development, 8, 69–86, https://doi.org/10.5194/gmd-8-69-2015, 2015.

Riley, G. A.: The relationship of vertical turbulence and spring diatom flowerings, Journal of Marine Research, 78, https://elischolar.library.yale.edu/journal_of_marine_research/495, 1942.

Rumyantseva, A., Henson, S., Martin, A., Thompson, A. F., Damerell, G. M., Kaiser, J., and Heywood, K. J.: Phytoplankton spring bloom initiation: The impact of atmospheric forcing and light in the temperate North Atlantic Ocean, Progress in Oceanography, 178, 102 202, https://doi.org/https://doi.org/10.1016/j.pocean.2019.102202, 2019.

Sathyendranath, S., Brewin, R., Brockmann, C., Brotas, V., Calton, B., Chuprin, A., Cipollini, P., Couto, A., Dingle, J., Doerffer, R., Donlon, C., Dowell, M., Farman, A., Grant, M., Groom, S., Horseman, A., Jackson, T., Krasemann, H., Lavender, S., Martinez-Vicente, V., Mazeran, C., Mélin, F., Moore, T., Müller, D., Regner, P., Roy, S., Steele, C., Steinmetz, F., Swinton, J., Taberner, M., Thompson, A., Valente, A., Zühlke, M., Brando, V., Feng, H., Feldman, G., Franz, B., Frouin, R., Gould, Jr., R., Hooker, S., Kahru, M., Kratzer, S., Mitchell, B., Muller-Karger, F., Sosik, H., Voss, K., Werdell, J., and Platt, T.: An ocean-colour time series for use in climate studies: the experience of the Ocean-Colour Climate Change Initiative (OC-CCI). Sensors: 19, 4285., Sensors, https://doi.org/doi:10.3390/s19194285, 2019.

Sathyendranath, S., Jackson, T., Brockmann, C., Brotas, V., Calton, B., Chuprin, A., Clements, O., Cipollini, P., Danne, O., Dingle, J., Donlon, C., Grant, M., Groom, S., Krasemann, H., Lavender, S., Mazeran, C., Mélin, F., Müller, D., Steinmetz, F., Valente, A., Zühlke, M., Feldman, G., Franz, B., Frouin, R., Werdell, J., and Platt, T.: ESA Ocean Colour Climate Change Initiative: Monthly climatology of global ocean colour data products at 4km resolution, Version 6.0., https://catalogue.ceda.ac.uk/uuid/690fdf8f229c4d04a2aa68de67beb733, 2023.

Saulter, A.: Atlantic- European North West Shelf- Wave Physics Reanalysis, https://doi.org/https://doi.org/10.48670/moi-00060, 2024.

Saulter, A., Bunney, C., Li, J.-G., and Palmer, T.: Process and resolution impacts on UK coastal wave predictions from operational global-regional wave models, in: 15th international workshop on wave hindcasting and forecasting & 6th coastal hazard symposium, vol. 10, p. 15, 2017.

Sharples, J., Moore, C. M., and Abraham, E. R.: Internal tide dissipation, mixing, and vertical nitrate flux at the shelf edge of NE New Zealand, Journal of Geophysical Research: Oceans, 106, 14 069–14 081, https://doi.org/https://doi.org/10.1029/2000JC000604, 2001.

Sharples, J., Ross, O. N., Scott, B. E., Greenstreet, S. P., and Fraser, H.: Inter-annual variability in the timing of stratification and the spring bloom in the North-western North Sea, Continental Shelf Research, 26, 733–751, https://doi.org/https://doi.org/10.1016/j.csr.2006.01.011, 2006.

Shi, W. and Wang, M.: Observations of a Hurricane Katrina-induced phytoplankton bloom in the Gulf of Mexico, Geophysical Research Letters, 34, https://doi.org/https://doi.org/10.1029/2007GL029724, 2007.

Simpson, D., Benedictow, A., Berge, H., Bergström, R., Emberson, L. D., Fagerli, H., Flechard, C. R., Hayman, G. D., Gauss, M., Jonson, J. E., Jenkin, M. E., Nyíri, A., Richter, C., Semeena, V. S., Tsyro, S., Tuovinen, J.-P., Valdebenito, A., and Wind, P.: The EMEP MSC-W chemical transport model - technical description, Atmospheric Chemistry and Physics, 12, 7825–7865, https://doi.org/10.5194/acp-12-7825-2012, 2012.

Simpson, J. H. and Sharples, J.: Introduction to the Physical and Biological Oceanography of Shelf Seas, Cambridge University Press, 2012.

Skákala, J., Bruggeman, J., Brewin, R. J. W., Ford, D. A., and Ciavatta, S.: Improved Representation of Underwater Light Field and Its Impact on Ecosystem Dynamics: A Study in the North Sea, Journal of Geophysical Research: Oceans, 125, e2020JC016 122, https://doi.org/https://doi.org/10.1029/2020JC016122, 2020.

Stokes, G. G.: On the theory of oscillatory waves, Transactions of the Cambridge Philosophical Society, 8, 441–455, 1847.

Sverdrup, H. U.: On Conditions for the Vernal Blooming of Phytoplankton, Journal du Conseil, 18, 287–295, https://doi.org/10.1093/icesjms/18.3.287, 1953.

Taylor, J. R. and Ferrari, R.: Shutdown of turbulent convection as a new criterion for the onset of spring phytoplankton blooms, Limnology and Oceanography, 56, 2293–2307, https://doi.org/https://doi.org/10.4319/lo.2011.56.6.2293, 2011.

Tensubam, C. M., Babanin, A. V., and Dash, M. K.: Wave-Coupled Effects on Oceanic Biogeochemistry: Insights From a Global Ocean Biogeochemical Model in the Southern Ocean, Earth and Space Science, 11, e2024EA003 748, https://doi.org/10.1029/2024EA003748, 2024.

825 Tolman, H.: The WAVEWATCH III Development Group: User manual and system documentation of WAVEWATCH III version 4.18, Technical Note, Environmental Modeling Center, National Centers for Environmental Prediction, National Weather Service, National Oceanic and Atmospheric Administration, US Department of Commerce, College Park, MD, 2014.

Tonani, M., Sykes, P., King, R. R., McConnell, N., Péquignet, A.-C., O'Dea, E., Graham, J. A., Polton, J., and Siddorn, J.: The impact of a new high-resolution ocean model on the Met Office North-West European Shelf forecasting system, Ocean Science, 15, 1133–1158,

830 https://doi.org/10.5194/os-15-1133-2019, 2019.

Uchiyama, Y., McWilliams, J. C., and Shchepetkin, A. F.: Wave–current interaction in an oceanic circulation model with a vortex-force formalism: Application to the surf zone, Ocean Modelling, 34, 16–35, https://doi.org/https://doi.org/10.1016/j.ocemod.2010.04.002, 2010.

Valcke, S., Craig, T., and Coquart, L.: {OASIS3}-{MCT} 3.0, 2015.

Valiente, N. G., Saulter, A., Edwards, J. M., Lewis, H. W., Castillo Sanchez, J. M., Bruciaferri, D., Christopher, B., and Siddorn, J.: The

835 Impact of Wave Model Source Terms and Coupling Strategies to Rapidly Developing Waves across the North-West European Shelf during Extreme Events, Journal of Marine Science and Engineering, 9, https://doi.org/10.3390/jmse9040403, 2021.

van Leeuwen, S., Tett, P., Mills, D., and van der Molen, J.: Stratified and nonstratified areas in the North Sea: Long-term variability and biological and policy implications, Journal of Geophysical Research: Oceans, 120, 4670–4686, https://doi.org/https://doi.org/10.1002/2014JC010485, 2015.

840 Virtanen, P., Gommers, R., Oliphant, T. E., Haberland, M., Reddy, T., Cournapeau, D., Burovski, E., Peterson, P., Weckesser, W., Bright, J., van der Walt, S. J., Brett, M., Wilson, J., Millman, K. J., Mayorov, N., Nelson, A. R. J., Jones, E., Kern, R., Larson, E., Carey, C. J., Polat, İ., Feng, Y., Moore, E. W., VanderPlas, J., Laxalde, D., Perktold, J., Cimrman, R., Henriksen, I., Quintero, E. A., Harris, C. R., Archibald, A. M., Ribeiro, A. H., Pedregosa, F., van Mulbregt, P., and SciPy 1.0 Contributors: SciPy 1.0: Fundamental Algorithms for Scientific Computing in Python, Nature Methods, 17, 261–272, https://doi.org/10.1038/s41592-019-0686-2, 2020.

845 Vörösmarty, C. J., Fekete, B. M., Meybeck, M., and Lammers, R. B.: Global system of rivers: Its role in organizing continental land mass and defining land-to-ocean linkages, Global Biogeochemical Cycles, 14, 599–621, https://doi.org/https://doi.org/10.1029/1999GB900092, 2000.

Waniek, J.: The role of physical forcing in initiation of spring blooms in the northeast Atlantic, Journal of Marine Systems, 39, 57–82, 2003.

Woollings, T., Hannachi, A., and Hoskins, B.: Variability of the North Atlantic eddy-driven jet stream, Q. J. R. Meteorol. Soc., 136, 856–868,

850 2010.

Young, E. F. and Holt, J. T.: Prediction and analysis of long-term variability of temperature and salinity in the Irish Sea, Journal of Geophysical Research: Oceans, 112, https://doi.org/https://doi.org/10.1029/2005JC003386, 2007.

Zhang, X., Simons, R., Zheng, J., and Zhang, C.: A review of the state of research on wave-current interaction in nearshore areas, Ocean Engineering, 243, 110 202, https://doi.org/https://doi.org/10.1016/j.oceaneng.2021.110202, 2022.

855 Zhang, Y., Sevault, F., Pennel, R., and Baklouti, M.: Analysis of the impact of vertical variation and temporal frequency of the chlorophyll forcing field on modelled temperature in the Mediterranean Sea and potential implications for regional climate projections, Ocean Modelling, 194, 102 490, https://doi.org/https://doi.org/10.1016/j.ocemod.2024.102490, 2025.

Øyvind Breivik, Mogensen, K., Bidlot, J.-R., Balmaseda, M. A., and Janssen, P. A. E. M.: Surface wave effects in the NEMO ocean model: Forced and coupled experiments, Journal of Geophysical Research: Oceans, 120, 2973–2992, https://doi.org/https://doi.org/10.1002/2014JC010565, 2015.

Øyvind Breivik, Bidlot, J.-R., and Janssen, P. A. E. M.: A Stokes drift approximation based on the Phillips spectrum, Ocean Modelling, 100, 49–56, https://doi.org/https://doi.org/10.1016/j.ocemod.2016.01.005, 2016.

860